Vector-Galileon-Tensor Theories of Gravity

Timothy Oreta
University of Cape Town (UCT)

Supervisor: $Prof.$ Peter Dunsby (University of Cape Town)

Co-supervisor: $Dr.$ José Beltrán Jiménez (Aix-Marseille University)

Department of Mathematics and Applied Mathematics, Faculty of Science,
University of Cape Town, South Africa

Submitted in partial fulfillment of the requirements of Master of Science (MSc.) degree

in Astrophysics and Space Science at the University of Cape Town, South Africa

April 6, 2016

Declaration

I, Timothy Oreta, hereby declare that the work on which this thesis is based is my original work (except where acknowledgements indicate otherwise) and that neither the whole work nor any part of it has been, is being, or is to be submitted for another degree in this or any other university. I authorise the University to reproduce for the purpose of research either the whole or any portion of the contents in any manner whatsoever.

Signature:..... Date:.....

Abstract

A detailed study of the cosmological evolution in a particular vector-tensor theory of gravity with a potential and a $Galileon$-motivated interaction terms is presented. The evolution of vector field self-interactions that are relatively related to $Galileon$ fields throughout the expansion history of the universe is considered and a classification of the parameters M (mass term) and H ($Hubble$ parameter) according to the behaviour of the field in each cosmological epoch is carried out. In particular, we obtain conditions for the parameters so that the field grows exponentially or oscillates with decreasing amplitude. We also obtain an autonomous system for the inflationary case. The general features of the phasemaps are given and the critical point is appropriately characterised. It is not possible to obtain an autonomous system for radiation and matter dominated epochs hence, we consider other analytical methods. We obtain eigenvalues and hence, phasemaps. The general features of the phasemaps are given and the point to which the trajectories on the phasemaps converge is appropriately characterised. Therefore, we show that it is possible to obtain a wide variety of behaviours or interesting phenomenologies for the cosmological evolution of vector field self-interactions that are relatively related to $Galileon$ fields by choosing suitable values for the parameters M and H of given conditions.

Keywords: Vector Field Self-Interactions, $Galileon$ Fields, Cosmological Evolution, Relatively Related.

Notations and Conventions:

The following notations are used in this thesis unless otherwise (specified). The metric signature is taken to be + - - - in four spacetime dimensions in chapter 3 while it is taken be - + + + in chapters 1 and 2. Units are used in which the speed of light c and the reduced $Planck$ constant $\hbar$ assume the value unity. G is $Newton's$ constant, the $Planck$ mass is $m_{pl} = G^{-\frac{1}{2}}$, while $\kappa \equiv 8\pi G = 1$. $Greek$ indices take the values 0, 1, 2, 3 and $Latin$ indices take the spatial values 1, 2, 3. A comma symbolises ordinary differentiation, ∇_a is the covariant derivative operator, and g symbolises the determinant of the metric tensor $g_{\mu\nu}$, while $\eta_{\mu\nu}$ is the $Minkowski$ metric, which assumes the form $diag(-1, +1, +1, +1)$ in chapter 1 in $Cartesian$ coordinates in four dimensions. $R \equiv g^{\alpha\beta}R_{\alpha\beta}$ is called the $Ricci$ curvature. The subscript 0 usually identifies quantities evaluated at the present epoch of time t in the history of the universe. For figures 3.1, 3.2, 3.7, 3.8, 3.10 and 3.11, the notation we use for the field is B..z(t)=B_z. For figures 3.9 and 3.12, the notation we use for the field is $B'_z = \dot{B}_z$.

$Timothy\ Oreta$

Acknowledgements

First, I would like to thank my mother for providing me with the opportunity to be where I am today. I thank my whole family for their encouraging words. Without my family, none of this would be possible.

I thank my supervisor $Prof.$ Peter Dunsby and co-supervisor $Dr.$ José Beltrán Jiménez, for their insightful guidance, direction and assistance. I thank $Prof.$ Peter Dunsby for his patience, kindness and sacrifices, enabling the completion of this thesis.

I thank the National Astrophysics and Space Science Programme ($NASSP$) who sponsored my education and assisted me in many ways. Of note in $NASSP$ is $Mrs.$ Nicky Walker who assisted me with all sorts of problems.

My gratitude also goes to all my friends especially Manana, Tony and Lorenzo who helped me with computational problems. I also thank anyone or everyone who took part in the development of this thesis but I have not mentioned.

Table of Contents

List of Figures

List of Tables

Chapter 1. Standard Cosmology

Cosmology (from the $Greek$: kosmos, universe, world, order, and logos, word, theory) is possibly the most ancient body of knowledge, dating from as far back as the predictions of seasons by early civilizations [94]. However, it was not until recently, that we could answer some of its more basic questions with an order of magnitude estimate [5, 49]. This primitive state of affairs has dramatically changed in the last few years, thanks to raw data, coming from precise measurements of a wide range of cosmological parameters [49].

Our current understanding of the universe is based on the hot big bang (BB) theory, which successfully explains its evolution from the first fraction of a second to our current age, which is about 14 billion years later [89]. This theory relies on four strong pillars, a theoretical framework based upon general relativity (GR), as put forward by $Albert\ Einstein$ [82] (he developed GR) and $Alexander\ A.\ Friedmann$ [36] (he led to the development of modern cosmology) in the $1920s$, and three robust observational facts: First, the discovery by $Georges\ Lemaître$ theoretically although widely attributed to $Edwin\ P.\ Hubble$ [82] (he proved it observationally) in the $1920s$, that the universe is expanding due to the recession of galaxies at a speed proportional to their distances from us. Second, the relative abundance of light elements, explained by $George\ Gamow$ [19] in the $1940s$. These are mainly helium, deuterium and lithium, which were produced from the nuclear reactions that took place at around a second to a few minutes after the BB, when the universe was a few times hotter than the core of the sun. Third, the afterglow of the BB called the cosmic microwave background (CMB), which was discovered in 1965 by $Arno\ A.\ Penzias$ and $Robert\ W.\ Wilson$ [26] as a very isotropic blackbody radiation at a temperature of about, $3K$ emitted when the universe was cold enough to form neutral atoms, and photons decoupling from matter, approximately $380,000$ years after the BB. Currently, these observations are confirmed to within a few percent accuracy, and have helped establish the hot BB as the preferred model of the universe.

1.1 The Homogeneous and Isotropic Universe

There are a huge variety of physical configurations in the universe [83]. One of them being Density, has been shown to have an average within a galaxy which is typically 10^5 larger than the

average Density of the universe [74]. It has also been shown that galaxies contain objects such as neutron stars which are much denser than the galactic average [83]. Hence, observing the universe at various length scales suggests that an average description on very large scales might be the simplified description we have been looking for [83]. The strongest evidence on the large scale isotropy of the universe comes from the isotropy of the CMB radiation. This radiation bath fills the whole universe. This implies that the observable universe is apparently (spatially) highly isotropic around us. It has also been shown that the number count of galaxies we see in the sky proves that the universe is homogeneous. When counting radio sources, we can detect observations of X-ray and γ-ray backgrounds and the smoothness $\left(\frac{\delta T}{T} \lesssim 10^{-5}\right)$ of the CMB radiation also confirms this [83].

However, in order to be successful in the construction of the model of the universe, the view should be both from planet earth and beyond [83] and at different times. More data about the universe is needed from other positions [83]. Since that is almost impossible in practice, some assumptions have been formulated [83]. It is reasonable to assume that we do not occupy a special position in the universe [83] although eventually this needs to be supported by data. This assumption is called the $Copernican$ principle [83]. This further shows that, on large scales, the observable universe is spatially homogeneous [83]. It can also be seen that isotropy from every point implies homogeneity [97]. This is verified $a\ posteriori$, by comparing the predictions of the model obtained that are based on observations and this is also very well verified by several different types of observations [108].

It is reasonable to start from the laws which explain physics very well on energies or length scales we can investigate on and around our planet (in a lab, or with high precision measurements in the solar system), and extrapolate their validity to different scales [83]. This way of advancing knowledge is not guaranteed to be correct, since new degrees of freedom or even new dynamical laws may show up as we increase the length scales and the complexity of the system under investigation [83]. Alternatively, it is a very sensible guess (if not the best) to start with [83]. Therefore, the correct set of concepts to use to model the universe is the one offered by GR [29], which is currently the best possible theory that explains correctly the gravitational interaction up to mm scales. Gravity is known to be the only force responsible for the large scale structure of the universe [83]. To be specific, we will study an extension of the original theory, proposed by $Einstein$, where the cosmological constant is clearly present in the equations of motion [70, 87].

In this structure, gravity is seen as a geometrical effect and the geometrical properties of the universe are encoded in the metric tensor $g^{\alpha\beta}$ where α and β are indices [83]. The curvature of

the universe is obtained from the energy-momentum tensor of matter fields $T^{\alpha\beta}$, and is determined by $Einstein's$ field equations (EFE) [83]:

$$G^{\alpha\beta} + \Lambda g^{\alpha\beta} = \frac{8\pi G T^{\alpha\beta}}{c^4}, \tag{1.1}$$

where, G is the $Newtonian$ constant, Λ is the so-called cosmological constant, c is the speed of light and $G^{\alpha\beta}$ is the $Einstein$ tensor.

1.1.1 The Friedmann-Lemaître-Robertson-Walker Metric

In order to describe the real world, we are forced to give up the perfect $Copernican$ principle, which implies symmetry throughout space and time [92]. It turns out to be straightforward, and consistent with observations, to propound that the universe is spatially homogeneous and isotropic [109], but evolving in time. In GR this is rephrased in the statement that the universe can be foliated into spacelike slices [84] such that each three-dimensional slice is maximally symmetric. Hence, we consider our spacetime $\overline{M}$ to be, $\overline{R} \times \Sigma$ where, $\overline{R}$ represents the time direction and, Σ is a maximally symmetric three-manifold [16]. The spacetime metric is therefore expressed in the form [16]:

$$ds^2 = -dt^2 + R(t)^2 d\sigma^2, \tag{1.2}$$

with, t as the timelike co-ordinate, $R(t)$ as a function known as the scale factor and, $d\sigma^2$ as the metric on, Σ which can be expressed as:

$$d\sigma^2 = \gamma_{ij}(u) du^i du^j, \tag{1.3}$$

where for, i=j=(1,2,3), (u^1, u^2, u^3) are coordinates on, Σ and, γ_{ij} is a maximally symmetric three-dimensional metric [16]. The scale factor tells us how big the spacelike slice, Σ is at the current time, t [16].

Maximally symmetric $Euclidean$ three-metrics, γ_{ij} are more relevant [16]. We know that maximally symmetric metrics must behave according to [16]:

$${}^{(3)}R_{ijkl} = k(\gamma_{ik}\gamma_{jl} - \gamma_{il}\gamma_{jk}), \tag{1.4}$$

where for future convenience we introduce:

$$k = \frac{^{(3)}R}{6}, \tag{1.5}$$

and the superscript, $^{(3)}$ on the $Riemann$ tensor is there to remind us that it is associated with the three-metric, γ_{ij} not the metric of the entire spacetime [16]. The $Ricci$ tensor would then be expressed in the form [16]:

$$^{(3)}R_{ij} = 2k\gamma_{jl}. \tag{1.6}$$

Spherical symmetry will cause the space to be maximally symmetric [16]. Equation 1.3 can be expressed in the form:

$$d\sigma^2 = \exp(2\beta(\overline{r}))d\overline{r^2} + \overline{r^2}d\Omega^2, \tag{1.7}$$

after using the $Schwarzschild$ solution of EFE expressed as:

$$ds^2 = -\left[1 - \frac{2M}{\overline{r}}\right]dt^2 + \frac{1}{1 - \frac{2M}{\overline{r}}}d\overline{r^2}d\theta^2 + \overline{r^2}\sin^2\theta d\theta^2, \tag{1.8}$$

where M is the mass and $\overline{r}$ is called the radial coordinate [16]. For equation 1.7 the metric on the two-sphere is, $d\Omega^2 = d\theta^2 + \sin^2\theta d\theta^2$ as usual [16]. When we work out the components we obtain [16]:

$$\begin{aligned} ^{(3)}R_{11} &= \frac{2}{\overline{r}}\partial_1\beta, \\ ^{(3)}R_{22} &= \exp[-2\beta][\overline{r}\partial_1\beta - 1] + 1, \\ ^{(3)}R_{33} &= [\exp(-2\beta)(\overline{r}\partial_1\beta - 1) + 1]\sin\theta. \end{aligned} \tag{1.9}$$

Substituting the metric into 1.6 we obtain:

$$\beta = -\frac{1}{2}\ln[1 - k\overline{r^2}], \tag{1.10}$$

hence, we can write:

$$d\sigma^2 = \frac{d\overline{r^2}}{1 - k\overline{r^2}} + \overline{r^2}d\Omega^2, \tag{1.11}$$

on the three-surface, Σ [16]. From equation 1.5 we can see that, k sets the curvature [16]. This

was then normalized to [16]:

$$k \in [+1, 0, -1]. \tag{1.12}$$

The $k = -1$ case would match to constant negative curvature on Σ, and is sometimes called open; the $k = 0$ case corresponds to no curvature on Σ, and is called flat; the $k = +1$ case corresponds to positive curvature on Σ, and is sometimes called closed [16]. These cases can be made more comprehensible by using an alternative form of the metric, obtained by introducing the new coordinate χ defined by [16]:

$$d\chi = \frac{d\overline{r}}{\sqrt{1 - k\overline{r}^2}}. \tag{1.13}$$

Integrating this results in:

$$\overline{r} = S_k(\chi), \tag{1.14}$$

where:

$$S_k(\chi) = \begin{cases} \sin(\chi) & \text{if } k = +1, \\ \chi & \text{if } k = 0, \\ \sinh(\chi) & \text{if } k = -1, \end{cases} \tag{1.15}$$

leading to:

$$d\sigma^2 = d\chi^2 + S_k^2(\chi) d\Omega^2, \tag{1.16}$$

[16]. For the flat case, $k = 0$ the metric on Σ would be expressed as:

$$\begin{aligned} d\sigma^2 &= d\chi^2 + \chi^2 d\Omega^2, \\ &= dx^2 + dy^2 + dz^2, \end{aligned} \tag{1.17}$$

which is simply flat $Euclidean$ space [16]. For a closed case, $k = +1$ we have the expression:

$$d\sigma^2 = d\chi^2 + \sin^2(\chi) d\Omega^2, \tag{1.18}$$

which is the metric of a three-sphere [16]. In this instance, the only possible global structure is

the complete three-sphere [16]. Finally, in the open, $k = -1$ case the result is [16]:

$$d\sigma^2 = d\chi^2 + \sinh^2(\chi) d\Omega^2. \tag{1.19}$$

This is the metric for a three-dimensional space of unchanging negative curvature [16]. Globally, such a space could extend for all future times, but it could also describe a non simply-connected compact space [16].

The metric on spacetime that describes one of these maximally-symmetric hypersurfaces can be expressed as [16]:

$$ds^2 = -dt^2 + R(t)^2 \left[\frac{d\overline{r^2}}{1 - k\overline{r^2}} + \overline{r^2} d\Omega^2 \right]. \tag{1.20}$$

This is known as the $Friedmann - Lemaître - Robertson\text{-}Walker$ $(FLRW)$ metric [58]. Note also that the substitutions below:

$$\begin{aligned} R &\to \lambda^{-1} R, \\ \overline{r} &\to \lambda \overline{r}, \\ k &\to \lambda^{-2} k, \end{aligned} \tag{1.21}$$

leave equation 1.20 unchanged [16]. A convenient normalization was then chosen [16]. In the variables where the curvature k is normalized to $[+1, 0, -1]$, the scale factor a has units of distance and the radial coordinate $\overline{r}$ (or χ) is actually dimensionless; this is the choice considered to be the best in this situation [16]. It is just more convenient to use a dimensionless scale factor expressed as:

$$a(t) = \frac{R(t)}{R_0(t)}, \tag{1.22}$$

a coordinate with dimensions of distance:

$$r = R_0 \overline{r}, \tag{1.23}$$

and a curvature parameter with dimensions of $(length)^{-2}$:

$$\kappa = \frac{k}{R_0^2} \tag{1.24}$$

[16]. Note that κ can take on just any given value, not just $[+1, 0, -1]$ [16]. In these variables,

the metric $FLRW$ can be expressed in the form [16]:

$$ds^2 = -dt^2 + a(t)^2\left[\frac{dr^2}{1-kr^2} + r^2 d\Omega^2\right]. \tag{1.25}$$

1.1.2 Perfect Fluids

For real fluids, each particle has some random (thermal) velocity and there may be different forces between the particles that contribute potential energies to the total besides the bulk motion of the fluids [16, 72, 99, 102]. The physical meaning of the components of the energy-momentum tensor $\overline{T}$ gives one an understanding on how to generalise its form to include these properties of real fluids [16, 72, 99, 102].

$\overline{T}$ at some event P was considered and work was done in a local $Cartesian$ inertial frame S (IRF) of the fluid at P [16, 72, 99, 102]. For dust, the only non-zero component is given by T^{00} [16, 72, 99, 102]. However, the components of $\overline{T}$ in the IRF for a real fluid was considered.

- T^{00} is the total energy density, including any potential energy contribution from forces in between the particles and kinetic energy from their random thermal motions [16, 72, 99, 102].
- T^{0i} [16, 72, 99, 102]: this represents the energy flow in the i-direction. Although there is no bulk motion, energy could be transferred by heat conduction. Therefore, this is basically a heat conduction term in the IRF.
- T^{i0} [16, 72, 99, 102]: this constitutes the momentum density in the i-direction. Although the particles have no bulk motion, the heat that would be conducted away will ensue in energy carrying momentum.
- T^{ij} [16, 72, 99, 102]: the random thermal motions of the particles will ensue momentum flow, so that T^{ij} is the isotropic pressure in the i-direction and the T^{ij} (with $i \neq j$) are the viscous stresses in the fluid.

These are all true for a general fluid [16, 72, 99, 102]. A perfect fluid is then defined as one for which there is no heat conduction or viscosity in the IRF [27]. This would mean that the

components of $\overline{T}$ for a perfect fluid in the IRF are given by

$$[T^{\alpha\beta}] = \begin{bmatrix} \rho & 0 & 0 & 0 \\ 0 & \mathsf{P} & 0 & 0 \\ 0 & 0 & \mathsf{P} & 0 \\ 0 & 0 & 0 & \mathsf{P} \end{bmatrix},$$

where ρ is the density and P is the pressure [27]. It is easy to show that this can be written as [27]:

$$T^{\alpha\beta} = [\rho + P]u^{\alpha}u^{\beta} + P\eta^{\alpha\beta}, \tag{1.26}$$

where [27]

$$[\eta^{\alpha\beta}] = \begin{bmatrix} -1 & 0 & 0 & 0 \\ 0 & 1 & 0 & 0 \\ 0 & 0 & 1 & 0 \\ 0 & 0 & 0 & 1 \end{bmatrix}.$$

and u^{α} or u^{β} is the four velocity. Equation 1.26 must be true in any IRF at P [16, 72, 99, 102]. An expression that is true in an arbitrary coordinate system can be obtained simply by replacing $\eta^{\alpha\beta}$ with the metric functions $g^{\alpha\beta}$ in the arbitrary system [16, 72, 99, 102]. A fully contra-variant expression for the components of the energy-momentum tensor of a perfect fluid is obtained and this is [16, 72, 99, 102]:

$$T^{\alpha\beta} = [\rho + P]u^{\alpha}u^{\beta} + Pg^{\alpha\beta}. \tag{1.27}$$

It can be discerned easily that $T^{\alpha\beta}$ is symmetric and is composed of the two scalar fields ρ and P and the vector field $\overline{u}$ that characterise the perfect fluid [16, 72, 99, 102]. It is not difficult to see that in the limit $P \to 0$ a perfect fluid becomes dust [16, 72, 99, 102].

1.1.3 Matter, Radiation and Vacuum

There are numerous physical systems in the universe that can be macroscopically explained as fluids [83]. Of particular importance in cosmology are perfect fluids which can have any equation of state. But we will consider only the equation of state $P = \rho\omega$, where P is pressure, ρ is density and ω is a constant [83]. For fluids with this equation of state, there are three special cases which require a more detailed description [83]: the cases for $\omega = 0$, $\omega = \frac{1}{3}$ and $\omega = -1$.

The case $w = 0$ is excellent for describing particles whose kinetic energy is negligible compared to their rest energy. This can be used to explain baryons and dark matter which constitutes galaxies. The case $w = \frac{1}{3}$ is best for describing particles whose rest energy is negligible with respect to their kinetic energy, such as radiation. A system like the electromagnetic field can be explained as a perfect fluid with the equation of state $P = \frac{\rho}{3}$. This is so because the energy-momentum tensor of the electromagnetic field is traceless, and is consistent with the idea that we might see the electromagnetic field as a collection of ultra-relativistic and massless photons. Finally, the case $w = -1$ can be used to describe vacuum energy. Quantum field theory shows that a vacuum state possesses non-zero energy: the contribution of a quantum field to classical energy-momentum tensor is expected to be the expectation value of the tensor $\hat{T_{\alpha\beta}}$. For flat space, the expectation value of the tensor $\hat{T_{\alpha\beta}}$ is proportional to $\eta_{\alpha\beta}$ provided that the quantum theory and the vacuum state are invariant with respect to $Lorentz$ transformations. This means that in curved spacetime the expectation value of the tensor $\hat{T_{\alpha\beta}}$ is proportional to $g_{\alpha\beta}$. It can be perceived that vacuum energy can be treated at semi-classical level as a perfect fluid with the equation of state $P = -\rho$. It is assumed that the cosmological constant is a second characteristic energy or length scale of the gravitational field which only shows up at ultra-large scales. It can then be thought of also as explaining the semi-classical effect of vacuum energy of quantum fields in the cosmological context. It would then be more logical to consider it as a source term, and move the cosmological constant term to the right hand side (RHS) of the EFE defining:

$$T^{(\Lambda)}_{\alpha\beta} = -\frac{\Lambda g_{\alpha\beta}}{8\pi G}. \tag{1.28}$$

This type of energy-momentum tensor is typified by a pressure $P = -\frac{\Lambda}{8\pi G}$ and an energy density given by $\rho = \frac{\Lambda}{8\pi G}$.

1.2 The Friedmann-Lemaître-Robertson-Walker Model

1.2.1 The Friedmann Equations

The $Friedmann$ equations can be obtained as shown in [36, 37]. Using the 00-component of EFE for equations 1.27 and 1.25 we obtain [69, 72, 102, 109]:

$$H^2 = \frac{8\pi G\rho}{3} - \frac{k}{a^2} + \frac{\Lambda}{3}. \tag{1.29}$$

Combining this equation with the trace of EFE for the $FLRW$ metric 1.25 we obtain:

$$H^2 = -\frac{4\pi G}{3}[\rho + 3P] + \frac{\Lambda}{3}. \tag{1.30}$$

The Hubble parameter H, can be defined as [60]:

$$H^2 = \left[\frac{\dot{a}}{a}\right]^2, \tag{1.31}$$

which can be re-expressed as:

$$H^2 = \frac{\ddot{a}}{a} - \dot{H}. \tag{1.32}$$

Considering the cosmological constant as a fluid with a constant energy density during the expansion of the universe results in:

$$\rho_\Lambda = \frac{\Lambda}{8\pi G}. \tag{1.33}$$

With this the $Friedmann$ equations can be re-expressed as:

$$\left(\frac{\dot{a}}{a}\right)^2 = \frac{8\pi G\rho}{3} - \frac{k}{a^2} + \frac{\Lambda}{3}, \tag{1.34}$$

or:

$$\frac{\ddot{a}}{a} = -\frac{4\pi G}{3}[\rho + 3P] + \frac{\Lambda}{3}, \tag{1.35}$$

where ρ and P are the total energy density and pressure of the universe respectively, including the cosmological constant contribution.

From these equations, it is then possible to define the critical energy density as:

$$\rho_c = \frac{3H^2}{8\pi G}. \tag{1.36}$$

This then represents the density with which we would have a spatially flat universe ($k = 0$). If the energy density were larger than this value, the universe would then be positively curved ($k = +1$); if it were smaller than this value, the universe would then be negatively curved ($k = -1$).

It is more useful to define the ratio of the absolute density of the universe to the critical energy

density. This ratio is known as the density parameter and is given by [69, 72, 102, 109]:

$$\Omega = \frac{\rho}{\rho_c}. \tag{1.37}$$

All density parameters have a zero subscript if they refer to the present time. With equation 1.37, the first $Friedmann$ equation 1.34 takes the form:

$$1 - \Omega = -\frac{k}{a^2 H^2}. \tag{1.38}$$

The density parameter would then be related to the spatial geometry of the universe by [69, 72, 102, 109]:

for an open universe : $\Omega < 1 \implies k = -1$,
for a flat universe : $\Omega = 1 \implies k = 0$,
for a closed universe: $\Omega > 1 \implies k = +1$.

The RHS of equation 1.38 is known as the curvature parameter given by:

$$\Omega_k = -\frac{k}{a^2 H^2}, \tag{1.39}$$

and its energy density is called the curvature density $\rho_k = -\frac{3k}{8\pi a^2 G}$.

The $Friedmann$ equations are independent. To solve these equations, we need a third equation which relates the density and pressure. This equation is called an equation of state (discussed briefly earlier) and is given by:

$$P = \omega\rho, \tag{1.40}$$

where in this case ω is a dimensionless number that depends on each component of the universe. In order to solve this, equations 1.34 and 1.35 were combined, obtaining the continuity equation, that it directly follows from the conservation of stress-energy tensor that:

$$\begin{aligned} \dot{\rho} &= -3\frac{\dot{a}}{a}[\rho + P], \\ &= -3\frac{\dot{a}}{a}\rho[1 + \omega]. \end{aligned} \tag{1.41}$$

The general solution for this equation were ω is constant is:

$$\rho \propto a^{-3(1+\omega)}. \tag{1.42}$$

The evolution of the universe is not straightforward because it contains various components (non-relativistic matter, radiation, a cosmological constant and more exotic components) with different equations of state. Fortunately, the energy density and the pressure for these components of the universe are additive. This means that the continuity and the $Friedmann$ equations can be solved separately as long as the different components do not interact [69, 72, 102, 109].

- Non-relativistic matter. In this state, $\omega = 0$ and the fluid has zero pressure. This will cause the matter density to evolve as $\rho_m \propto a^{-3}$. It was then inferred that the energy density associated to non-relativistic matter decreases as the universe expands in proportion to its volume.

  Considering a spatially flat universe, it is then also possible to solve the $Friedmann$ equation obtaining the temporal evolution of the scale factor [69, 72, 102, 109]:

$$a(t) \propto t^{\frac{2}{3}}. \tag{1.43}$$

- Relativistic matter. For a universe that is dominated by radiation, $\omega = \frac{1}{3}$, and the energy density evolves as $\rho_r \propto a^{-4}$. In this state, for $k = 0$, the temporal evolution of the scale factor is:

$$a(t) \propto t^{\frac{1}{2}}. \tag{1.44}$$

- Vacuum energy. If the universe is dominated by a cosmological constant, $w = -1$ and $P_\Lambda = -\rho_\Lambda$. For a spatially flat universe, the scale factor a evolves as:

$$a(t) \propto \exp(Ht). \tag{1.45}$$

- More generally, for a universe with arbitrary k and having three components, that is, matter, radiation and a cosmological constant, the total density is given by [69, 72, 102, 109]:

$$\rho(a) \quad = \quad \rho_c^0[\Omega_m^0 a^{-3} + \Omega_r^0 a^{-4} + \Omega_\Lambda^0], \tag{1.46}$$

where:

$$\Omega_m^0 = \frac{8\pi G\rho_m^0}{3H_0^2c^2}, \Omega_r^0 = \frac{8\pi G\rho_r^0}{3H_0^2c^2}, \Omega_\Lambda^0 = \frac{\Lambda c^2}{3H_0^2}. \tag{1.47}$$

It follows that we can derive the time dependence of the $Hubble$ function from the $Friedmann$ equation given as [69, 72, 102, 109]:

$$H^2 = H_0^2[\Omega_k^0 a^{-2} + \Omega_m^0 a^{-3} + \Omega_r^0 a^{-4} + \Omega_\Lambda^0]. \tag{1.48}$$

Also the density parameters obey the following relation [42]:

$$1 = \Omega_m + \Omega_r + \Omega_\Lambda + \Omega_k. \tag{1.49}$$

1.2.2 The Expanding Universe

We have derived the equations that describe an expanding isotropic gas. They are the $Friedmann$ equation 1.34 which steers the time evolution of the scale factor $a(t)$, and the fluid equation 1.41, which gives us the evolution of the mass density $\rho(t)$. These are the real equations used by cosmologists, more traditionally obtained via the equations of GR.

We can now study two of their innuendos.

Hubble Law and Redshift

We can consider two variables related to the scale factor a: the $Hubble$ parameter and redshift [69, 72, 102, 109].

The $Hubble$ parameter [69, 72, 102, 109]:

$$\begin{aligned} H(t) &= \frac{1}{a}\frac{da}{dt}, \\ &= \frac{\dot{a}}{a}, \end{aligned} \tag{1.50}$$

measures how fast the scale factor a changes. The value of this parameter estimated at the present time ($Hubble$ constant) is known to great accuracy. Recent results from $Planck$, provides a value of $H(t_0) = H_0 = 67.8 \pm 0.9 kms^{-1}Mpc^{-1}$ [1].

At low redshift, this constant connects the recessional velocity of galaxies and their distance from their observer by the $Hubble$ law [69, 72, 102, 109]:

$$v = H_0 d, \tag{1.51}$$

where d is the distance of an object from us.

It is conventional to parametrise H_0 as:

$$H_0 = 100h\frac{km}{sMpc}, \tag{1.52}$$

where $h \sim 0.7$.

The redshift of a luminous source can be defined by the quantity:

$$z = \frac{\lambda_0 - \lambda_e}{\lambda_e}, \tag{1.53}$$

where λ_0 is the wavelength of the radiation from the source observed at O, that we assume to be the origin of our coordinate system, at time t_0; λ_e is the wavelength emitted at time t_e by the source which is at a comoving co-ordinate r. It is possible to derive the connection between the redshift and the scale factor a.

As it travels from the source to the observer, the radiation propagates along the null geodesics $ds^2 = 0$ and therefore, we have:

$$dt = -a(t)\frac{dr}{\sqrt{1-kr^2}}. \tag{1.54}$$

The light ray that is emitted from the source at time t_e reaches the observer at time t_0 therefore, we write:

$$\int_{t_e}^{t_0} \frac{dt}{a(t)} = -\int_{r1}^{0} \frac{dr}{\sqrt{1-kr^2}}. \tag{1.55}$$

The subsequent light ray that is emitted at time t_e+dt_e will be observed at time t_0+dt_0 satisfying:

$$\int_{t_e+dt_e}^{t_0+dt_0} \frac{dt}{a(t)} = -\int_{r1}^{0} \frac{dr}{\sqrt{1-kr^2}}. \tag{1.56}$$

Given that equation 1.55 does not change because r is a comoving coordinate and both the

source and the observer are moving with the cosmological expansion, equations 1.55 and 1.56 can be combined resulting in:

$$\int_{t_e+dt_e}^{t_0+dt_0} \frac{dt}{a(t)} = \int_{t_e}^{t_0} \frac{dt}{a(t)}, \tag{1.57}$$

from which we then derive:

$$\frac{dt_e}{a(t_e)} = \frac{dt_0}{a(t_0)}. \tag{1.58}$$

In particular, when we consider the frequencies of the emitted and observed light, $\nu_e = \frac{1}{dt_e}$ and $\nu_0 = \frac{1}{dt_0}$, we will have:

$$\nu_e a(t_e) = \nu_0 a(t_0), \tag{1.59}$$

or equivalently:

$$\frac{a(t)}{\lambda_e} = \frac{a(t_0)}{\lambda_0}. \tag{1.60}$$

Using equation 1.53, it was found that the relation between redshift and the expansion factor is:

$$1 + z = \frac{a(t_0)}{a(t_e)}. \tag{1.61}$$

Here the convention that $a(t_0) = a_0 = 1$ is used [69, 72, 102, 109]. This implies that the redshift observed for a distant object depends only on the relative scale factor at the time of emission.

The Expansion of the Universe and Thermodynamics

The three-dimensional velocity v^i for the free motion of massive particles in the $FLRW$ spacetime expressed in the comoving reference is called peculiar velocity [83]. This term is motivated by the fact that v^i is the excess (spatial) velocity of the test particle compared to the isotropic observers' one (which is zero in the comoving reference) [83]. Stipulating that $|\overline{v}|^2 = g_{ij}v^i v^j$, it can be showed [16] that the geodesic equation implies $|\overline{v}| \propto \frac{1}{a(t)}$.

This means that, if the scale factor is increasing (and so the universe is expanding), the peculiar velocity of a particle kinematically decreases and eventually becomes very small while the opposite would happen if the universe is contracting [83]. In particular, a perfect gas of particles in thermal

equilibrium in an expanding universe will get cooler, since its temperature is proportional to the average energy per degree of freedom [83]. Expansion leads to cooling, which is more generally true for a collection of interacting gases of particles, including a gas of massless particles (photons and neutrinos), apart possibly during phase transitions when energy and entropy are released into the system [83].

Conceptually, a $FLRW$ universe can never be in thermal equilibrium, since it is not stationary (in other words, the metric does not possess a time-like killing vector field) [83]. However, if the interactions between various species occur rapidly enough compared to the timescale of the expansion, the universe will to a good approximation evolve through a succession of nearly thermal equilibrium states [83]. The temperature then decreases as the scale factor increases [83]. Naively, a reaction is occuring rapidly enough to maintain the thermal equilibrium if its interaction rate Γ is satisfied [55] where:

$$\Gamma \gtrsim H, \tag{1.62}$$

with H as the $Hubble$ parameter. If certain types of particles are in thermal equilibrium with the other species (the thermal bath) and at a certain point its interaction rate decreases to the point that equation 1.62 is not satisfied, it can be said that it decouples from the thermal bath [83]. Particularly, as can be inferred by equation 1.59, a gas of non-interacting massless particles after decoupling maintains a thermal spectrum forever with temperature kinematically decreasing as $T \propto \frac{1}{a}$ [83].

The Universe in Thermal Equilibrium

According to the standard hot BB model, the early universe is well described by a state of thermal equilibrium. In fact, the interactions amongst the constituents of the primordial plasma should have been so effective that nuclear statistical equilibrium was achieved. This makes the study simple because the system may be fully described (neglecting chemical potentials for the time being) in terms of its temperature T. In a radiation dominated era the energy density and pressure are given by $\rho = 3P = \frac{\pi^2 g_* T^4}{30}$, where T dependent g_* gives the effective number of distinct helicity states of bosons plus fermions with masses $\ll T$. For particles with masses that are much larger than T (in natural units) the density in equilibrium is suppressed exponentially [see for example, [99]; the notation is borrowed from [55]].

The density in each component diminishes due to expansion and so it is harder for the above mentioned effective interaction rate Γ to keep working as before and hence, will fall below the

expansion rate. It is clear that there will be a point at which the interaction rate Γ will fall below the typified expansion rate. The temperature at that moment when the interaction rate of a species is said to decouple from the thermal fluid is called the decoupling temperature T_{dec}.

Let us now consider the history of the universe backwards in time. Early on, all matter in the universe was ionised and radiation was the dominant component. Owing to the expansion, the temperature cools down below $\sim$13.6eV and the recombination of electrons and protons to form hydrogen takes place, which diminishes the abundance of free electrons, making $Compton$ scattering not so effective. This results in the decoupling of the CMB radiation from matter and this (assuming the universe is matter-dominated at this time) occurs at approximately $t_{dec} \sim 5.6 \times 10^{12}(\Omega h^2)^{-\frac{1}{2}} s$. The analogous redshift is approximately $z_{dec} \simeq 1,100$ and the temperature $T_{dec} \simeq 3,000K = 0.3eV$.

Going still backwards in time the redshift $z_{eq} \simeq 2 \times 10^4 \Omega h^2$ when matter and radiation (i.e. very light particles) densities can be compared, the universe was $t_{eq} \simeq 1.4 \times 10^3 (\Omega h^2)^{-2}$ years old, with a temperature $T_{eq} \simeq 5.5 \Omega h^2 eV$ and density $\rho_{eq} \simeq 3.2 \times 10^{-16} (\Omega h^2)^4 g/cm^3$.

At earlier times densities and temperatures high enough for the production of the lightest elements was reached: when the age of the universe was between 0.01s and 3 minutes and its temperature was around $10 - 0.1MeV$, the synthesis of, D, ^3He, ^4He, ^7Li took place. The calculation of the abundance of these elements from cosmological origin is among the most useful analysis of the standard hot BB model (and certainly the earliest probe one can attain)[refer to [61]].

1.2.3 The Expansion History of the Universe

The, BB model provides one with a fairly comprehensible picture of how the universe evolved with time [72, 102, 109]. The key events in the expansion history of the universe are [72, 102, 109]:

- 10^{-4}s: Formation of photons and neutrons;
- 1s : Formation of light nuclei, via the nucleosynthesis process;
- 10^4s : The universe reaches the matter-radiation equality state;
- 10^5s : Formation of the, CMB owing to the decoupling of radiation from matter. This is coincident with the recombination epoch, when free electrons combine with nuclei to form atoms, and
- 10^{10} years : The current universe.

Theoretical support for the, BB theory is derived from the, $FLRW$ model, which explains the consistency of the, BB theory with, GR [72, 102, 109]. The hot, BB theory has been immensely successful in correlating the observable properties of our universe [72, 102, 109].

The Evolution of the Scale Factor

At low redshifts, one can develop, $a(t)$ in $Taylor$ series as:

$$\begin{aligned} a(t) &= a(t_0) + a(\dot{t_0})(t-t_0) + \frac{1}{2}a(\ddot{t_0})(t-t_0)^2 + ..., \\ a(t) &= a_0\left[1 + H_0(t-t_0) - \frac{1}{2}q_0H_0^2(t-t_0)^2 + ...\right], \end{aligned} \tag{1.63}$$

with:

$$q_0 = -\frac{\ddot{a_0}a_0}{\dot{a_0^2}} = \frac{\Omega_m}{2} - \Omega_\Lambda, \tag{1.64}$$

where we have used the fact that radiation is negligible at low redshifts z. With, $1+z = \frac{a_0(t)}{a(t)}$ one can write this as an expression for the lookback time as a function of redshift:

$$H_0[t_0 - t] = z - \left[1 + \frac{q_0}{2}\right]z^2 + ... \tag{1.65}$$

For example, for an $Einstein\text{-}de\ Sitter$ universe, which has, $\Omega_{total} = 1 = \Omega_m$ where, $H_0 = \frac{2}{3t_0}$ and $q_0 = \frac{1}{2}$:

$$\frac{t_0 - t}{t_0} = \frac{3}{2}\left[z - \left(1 + \frac{1}{4}\right)z^2 + ...\right], \tag{1.66}$$

so that at, $z = \frac{1}{2}$, $t_{\frac{1}{2}} = \left[\frac{23}{32}\right]t_0$ or approximately $\frac{1}{3}$ of the age of the universe which is below $z = \frac{1}{2}$.

The more general expression is obtained from $\dot{a} = aH(a)$ hence, $dt = \frac{da}{aH(a)}$ and therefore:

$$H_0t = H_0\int_0^a \frac{da}{\dot{a}} = \int_0^a \frac{da}{aE(z)} = \int_z^\infty \frac{dz}{(1+z)E(z)}, \tag{1.67}$$

where:

$$E(z) \quad = \quad [\Omega_m(1+z)^3 + \Omega_r(1+z)^4 + \Omega_k(1+z)^2 + \Omega_\Lambda]^{\frac{1}{2}}. \tag{1.68}$$

Here, t is the age of the universe at redshift z. For $z = 0$ and $t = t_0$:

$$H_0 t_0 \quad = \quad H_0 \int_0^{a_0} \frac{da}{\dot{a}} = \int_0^{\infty} \frac{dz}{(1+z)E(z)}. \tag{1.69}$$

Since the universe is not empty, $\Omega_m > \Omega_r > 0$ and this integral converges for, $z \to \infty$ which implies that the age of the universe is finite, at least if the physics we are using here applies all the way to infinity. This is not necessarily the case: we know that the laws of physics break down at sufficiently close to the BB. However, this should only happen at extremely high energies, long before there were stars, say. So t_0 should better be bigger than the age of the oldest stars we could find in the entire universe. For a long time, when people used to assume that, $\Omega_m = 1$ mostly because of theoretical prejudice, this was only marginally, and sometimes not even, fulfilled: some globular cluster stars were older (as judged from stellar evolution modelling) than the universe. The ages of these stars have been determined, whereas the discovery of the cosmological constant has increased, t_0 and there is no longer a problem.

Successes of the Standard Cosmological Model

The standard model of cosmology [69], [72] claims to have the least amount of speculatory inputs into cosmology, while having maximum agreement with observations. Some major success stories of the model can be discussed, collocating them with the current status of observational cosmology.

The discovery of a linear redshift-distance relation for galaxies by $Hubble$, if interpreted as due to $Doppler$ effect, establishes the case for an expanding phase for the universe at present and was a primary piece of evidence in support of the standard model of cosmology [69, 72, 102, 109]. Currently, the expansion rate, characterised by the $Hubble$ parameter 1.50 is in the range, $H_p = 100hkms^{-1}Mpc^{-1}$, $h = 0.68 \pm 0.9$ (The subscript p refers to the present epoch). The $Hubble$ radius H_p^{-1} gives a measure of the size of the currently observed universe. The deceleration parameter defined as:

$$\frac{\ddot{a}}{a} \quad = \quad -q(t)H(t)^2, \tag{1.70}$$

is estimated to be lying in the range $-0.55 < q_p < 2$. Also the density parameter, as per present

estimate is given by $0.1 \leq \Omega_p \leq 2$. The age of the universe, measured by direct observational dating techniques is around $t_p \approx 14$ billion years. Although these observations are approximate, they however, confirm the $Hubble$ expansion of the universe.

The observed redshift z of galaxies can be related to the scale factor as:

$$\frac{a(t_p)}{a(t_1)} = 1 + z, \tag{1.71}$$

where t_1 is the time at which the light is emitted. Assuming that the universe is composed of both radiation and matter, according to equation 1.42, before some time t_{eq} in its history, radiation will dominate over matter. In standard cosmology, t_{eq} is approximated to be $\approx 1.35 \times 10^{11} \Omega^{-\frac{3}{2}} h^{-3} s$. For a universe with flat space sections (i.e., $k = 0$), the following equation:

$$a(t) \propto t^{\frac{2}{3(1+w)}}, \tag{1.72}$$

derived by using equation 1.42 in 1.34 gives $a \propto t^{\frac{1}{2}}$ for the relativistic era and $a \propto t^{\frac{2}{3}}$ for the non-relativistic era. Assuming that the change is instantaneous, this results in:

$$a = At^{\frac{2}{3}}, t > t_{eq}, \tag{1.73}$$

and:

$$a = Bt^{\frac{1}{2}}, t < t_{eq}. \tag{1.74}$$

Matching the two relations at $t = t_{eq}$ results in:

$$\frac{B}{A} = \frac{t_{eq}^{\frac{2}{3}}}{t_{eq}^{\frac{1}{2}}} \approx 0.7 \times 10^2 \Omega^{\frac{-1}{4}} h^{\frac{-1}{2}} s^{\frac{1}{6}}. \tag{1.75}$$

This value will be valuable in evaluating expressions of the type 1.71 in the standard flat models. In the other cases with, $k = \pm 1$ the universe is regarded as nearly flat for smaller values of a_q by a few orders of magnitude.

Another important milestone in the development of the standard cosmological model was the discovery of the CMB radiation by $Penzias$ and $Wilson$ in 1965 [69, 72, 102, 109]. The spectrum of CMB radiation is consistent with that of a blackbody at the temperature $T_p \approx 2.73K$. It endorses the view that there was a more contracted state for the universe, which should have been denser and hotter than today. According to the standard model, the universe

cools as it expands and when the temperature reaches, $T \approx 4,000K$ matter ceases to be ionised. Radiation is then said not to be in thermal equilibrium with matter (matter-radiation decoupling) and the opacity of the radiation drops sharply. The radiation seen now as CMB radiation is devised as the relic of that last scattered at the time of decoupling. In fact, the CMB radiation was predicted by $Gamow$ in 1948 and its discovery, perhaps, is the strongest observational evidence in support of the standard model.

One can derive an expression for the total relavistic matter (radiation) density $\rho_{m,r}$ in terms of temperature. Using conventional units, for an ideal gas, there are $\frac{1}{\hbar^3}$ number of states situated in unit volume of μ-space say, where $\hbar$ is $Planck's$ constant. The number of states in volume V with momentum less than P is then given by $\left[\frac{4}{3}\right]\pi P^3 \frac{V}{\hbar^3}$. The occupancy of a single state is $\frac{1}{\exp\left(\frac{(E_A(P)-\mu_A)}{kT_A}\right)\pm 1}$. $\pm$ signs represent $Fermi(Bose)$ statistics, μ_A is the chemical potential and T_A is the temperature of the species A which is assumed to be in equilibrium and:

$$E_A(P) = [p^2c^2 + m^2c^4]^{\frac{1}{2}}, \tag{1.76}$$

the energy of a particle in the species A. The number of particles of type A with momentum between P and $P + dP$ per unit volume of space would then be:

$$n_A(P)dP = \frac{g_A P^2 dP}{2\pi^2\hbar^3 \exp\left(\frac{(E_A(P)-\mu_A)}{kT_A}\right) \pm 1}, \tag{1.77}$$

where g_A is the number of spin degrees of freedom. In the extreme relativistic ($T_A \gg m_A$) and nondegenerate ($T_A \gg \mu_A$) limit, the energy density, which corresponds to species A is given by:

$$\rho_A = \int_0^\infty E_A(P)n_A(P)dP = g_A\sigma T_A^4(Bosons), \tag{1.78}$$

$$\rho_A = \int_0^\infty E_A(P)n_A(P)dP = \left[\frac{7}{8}\right] g_A\sigma T_A^4(Fermions), \tag{1.79}$$

where $\sigma = \frac{\pi^2 k^4}{30\hbar^3 c^3} = 3.78 \times 10^{-15} ergsm^{-3}K^{-4}$. The total energy density contributed by all the relativistic species together can be written as shown below:

$$\rho_{m,r}c^2 = g_{total}\sigma T^4, \tag{1.80}$$

where:

$$g_{total} = \sum_{[A=Bosons]} g_A \left[\frac{T_A}{T}\right]^4 + \sum_{[A=Fermions]} \left[\frac{7}{8}\right] g_A \left[\frac{T_A}{T}\right]^4, \tag{1.81}$$

is the effective number of spin degrees of freedom at temperature T. In the very early universe, g_{tot} is shown to be almost equal to 100.

The expression for $\rho_{m,r}$ as given by equation 1.80 is a reasonable guess if we agree to look upon the CMB radiation as the relic of a hot early universe. To obtain another useful result in the study of the thermal history of an expanding universe, one can apply the second law of thermodynamics, in its familiar form, to a physical volume $V = a^3$;

$$\begin{aligned} kTds &= dE + PdV, \\ &= d[\rho c^2 a^3] + Pd[a^3], \end{aligned} \tag{1.82}$$

and also use:

$$\frac{d[\rho a^3]}{da} + 3Pa^2 = 0, \tag{1.83}$$

which is a statement of the first law of thermodynamics. It is easy to show that:

$$\begin{aligned} \frac{ds}{dt} &= \frac{1}{kT}\left[\frac{d}{dt}(\rho c^2 a^3) + P\frac{d}{dt}(a^3)\right], \\ &= 0. \end{aligned} \tag{1.84}$$

This means that the entropy per comoving volume element of unit coordinate volume, $V = a^3$ under thermal equilibrium, is a constant given by:

$$\begin{aligned} S &= \frac{[\rho c^2 + P]a^3}{kT}, \\ &= constant. \end{aligned} \tag{1.85}$$

Thus in the standard model, the universe expands adiabatically. Equation 1.80 implies that for radiation with, $\rho_{m,r} \propto a^{-4}$, aT is unchangeable. In the relavistic era, for a $k = 0$ universe, this may be used to express:

$$t = \left[\frac{3c^2}{32\pi G\sigma}\right]^{\frac{1}{2}} g_{tot}^{-\frac{1}{2}} T^{-2}. \tag{1.86}$$

The times at which radiation reaches various temperatures can be calculated using this formula.

The third important success of the standard model is the prediction of primordial nucleosynthesis [69], [72], [82], [99]. From this theory we learn that, when the age of the universe was about, $1s$ the temperature was of the order of $10^{10}K$ and the conditions were right for nuclear reactions which ultimately led to the production of significant amounts of D, ^3He and ^7Li. The yields of these light elements, according to the standard cosmological model, depends on the baryon to photon ratio η and the number of very light particle species, usually quantified as the equivalent number of light neutrino species N_ν. The predictions of the abundance of the above four light elements concur with the observational data provided the free parameters, η and, N_ν in the theory have values in the range given below:

$$2.5 \times 10^{-10} \leq \eta \leq 6.0 \times 10^{-10}, N_\nu \leq 3.9. \tag{1.87}$$

In turn, if we do accept the current abundance of light nuclei, the density parameter for baryons Ω_B may be predicted from the above to be lying in the range:

$$0.010 \leq \Omega_B \leq 0.15, \tag{1.88}$$

which agrees with measured values [90]. Furthermore, the bounds on, N_ν:

$$N_\nu \quad = \quad 3.0 \pm 0.020, \tag{1.89}$$

are in agreement with particle accelerator experiments [98].

1.3 The Late Time Acceleration Problem

The ΛCDM Model

The Λ-cold dark matter ($\Lambda\ CDM$) model is the best fit [21] model to several various cosmological observables and is a model of the late-time universe well after, BB nucleosynthesis. It explains a spatially flat universe composed of baryons, cold dark matter (CDM), radiation and a cosmological constant [69, 72, 102, 109]. Including these components and using the solution

to the continuity equation given below:

$$\rho = \frac{\rho_0}{a^{3(1+\omega)}}, \omega \neq -1, \tag{1.90}$$

or:

$$\rho = \rho_0, \omega = -1, \tag{1.91}$$

with, ρ_0 as the present day density, one can write the $Friedmann$ equation 1.29 in the form:

$$H^2 = H_0^2 \left[\frac{\Omega_c^0 + \Omega_b^0}{a^3} + \frac{\Omega_\gamma}{a^4} + \Omega_\Lambda \right], \tag{1.92}$$

where, c refers to CDM, b to baryons and, γ to radiation [69, 72, 102, 109]. The details of the very early universe are not important for the work explained later and so we assume that the universe exists from inflation (or some other early universe process) with a scale-invariant power spectrum and leave the processes of reheating and preheating unspecified. At this time, a is very small [6] and the radiation term dominates leading to an era that is dominated by radiation. As the scale factor a grows, the baryons and dark matter come to dominate leading to a matter dominated era [30] that begins at a redshift of about $z \sim 3,300$. Decoupling of photons and baryons happen at a redshift of about $z \sim 1,100$ in the matter dominated epoch. Finally, as these dilute and the scale factor continues to grow, only the cosmological constant is left and this dominates the subsequent evolution of the universe. The solutions of equation 1.92 deep in each of these eras so that the other terms can truly be neglected are:

$$a(t) = \left[\frac{t}{t_0} \right]^{\frac{2}{3}}, \tag{1.93}$$

for matter domination, or:

$$a(t) = \left[\frac{t}{t_0} \right]^{\frac{1}{2}}, \tag{1.94}$$

for radiation domination, or:

$$a(t) = \exp\left(\frac{\Lambda t}{3} \right), \tag{1.95}$$

for Λ domination where t_0 is the time today or the age of the universe [69, 72, 102, 109].

Many interesting cosmological probes including the, CMB radiation arise due to departures from the homogeneous and isotropic background in the form of linear perturbations [69, 72, 102, 109]. Linear perturbation theory in, GR and cosmology is a wide and interesting subject but we will not fully consider it.

1.3.1 The Composition of Our Universe

Some cosmological parameters can be approximated observationally [102] by comparing the theoretical predictions with observational data. The observational estimation of these parameters has recently become a very active field of research [76]: on one hand this is because the theoretical framework just described is flexible enough to account for different kinds of observations, but at the same time simple enough to allow its predictions to be tested with precision. On the other hand, it is due to the fact that the amount and precision of observational data has recently reached an unprecedented level. It is also quite involving technically hence, one gives into just following the basic underlying ideas.

Observations and Cosmological Parameters

It appears that the universe is expanding and thus, that, $a(t)$ is presently an increasing function with time [69, 72, 102, 109]. The recession speed of distant galaxies was first observed by $Slipher$ (1917) but $Lemaître$ was the first to postulate a linear relation between the recession speed v and distance x [69, 72, 102, 109]. This is exactly what one would expect from a universe conforming to the assumption behind the $Friedmann$ metric which for nearby objects the metric predicts that:

$$v = H_0 x, \tag{1.96}$$

so that the constant of proportionality between recession velocity v and distance x is the present day value of the $Hubble$ parameter-the $Hubble$ constant [69, 72, 102, 109]-a misnomer given that it changes with time (albeit slowly when compared with human timescales). The units of, H_0 set the typical time and length scales for the universe, within factors of, c, which are often

useful when computing physical quantities in cosmology:

$$\frac{1}{H_0} \approx 3,000 h^{-1} Mpc,$$
$$\frac{1}{H_0} \approx 9.8 h^{-1} Gyr. \tag{1.97}$$

Due to uncertainties in the measurement of the exact value of, H_0 it is usual to write, H_0 in terms of a small constant, h [69, 72, 102, 109], of order one. Hence, $H_0 = 100 h kms^{-1} Mpc^{-1}$. By examining equation 1.96 one could be forgiven for thinking that the distance and recession velocity of a single galaxy would be sufficient to measure, H_0. However, galaxies have unique velocities in addition to that from the $Hubble$ flow and so measurements of the recession velocities of a census of galaxies over a representative volume of the universe is necessary in order not to be biased by local flows. Some very close galaxies, such as $Andromeda$ ($0.8 Mpc$) and some satellites and dwarf galaxies have negative redshifts-meaning they are moving towards us. In some sense our position in the universe is lucky. The local peculiar velocities seem too low (the local $Hubble$ flow is quite smooth), which is probably due to the fact that we do not live near a massive galaxy cluster and so the $Hubble$ law is easier to measure locally. By attempting to measure absolute distance and velocity, a number of local measurements of, H_0 have been made. These depend primarily on being able to accurately determine the distance to galaxies.

Distances can be measured by different methods including the method of using the angular extent of an object. This can be done for objects like, $SN1987a$ where the angular extent of the supernova ejecta is measured along with the expansion velocity of the ejecta. Together, this permits the distance to the supernova to be accurately measured and this then provides an accurate distance to the Large Magellanic Cloud (LMC) galaxy. The, LMC contains a large population of stars called cepheid variables for which a tight relationship exists between the period of their luminosity oscillations (these are post main sequence stars with unstable outer layers) and the luminosity itself. It then follows that by measuring the period, the luminosity can be inferred and thus, a distance inferred by measuring the received flux. $Hubble$ in 1929 used cepheids to evaluate distances in the original work that showed the universe to be expanding.

If the universe does not have the critical density, then it would be sensible to include the spatial curvature term. Also, the vacuum energy may be non-zero. We divide the density into its matter, radiation, and vacuum components $\rho = \rho_m + \rho_r + \rho_{vac}$ respectively, and likewise for the density parameter, $\Omega = \Omega_m + \Omega_r + \Omega_\Lambda$ where, $\Omega_m = \frac{\rho_m}{\rho_c}$, $\Omega_r = \frac{\rho_r}{\rho_c}$ and $\Omega_\Lambda = \frac{\rho_{vac}}{\rho_c} \equiv \frac{\Lambda}{3H^2}$ with ρ_c as the critical density and Λ as the cosmological constant [42]. Ω_m, Ω_r and, Ω_Λ are functions of time (although, ρ_{vac} is a constant).

The, $FLRW$ cosmological model is defined by the present values of the cosmological parameters, H_0, Ω_m and, Ω_Λ [69, 72, 102, 109]. Observations favor the values, $h \sim 0.7$, $\Omega_m \sim 0.3$ and, $\Omega_\Lambda \sim 0.7$ [69, 72, 102, 109].

1.3.2 The Acceleration Problem

The, ΛCDM model (a widely agreed model) is very satisfactory since it gives a consistent description of all the cosmological observations [83]. The observed values of the cosmological parameters imply that the universe is currently vacuum dominated and its expansion is accelerating [83]. Just over 70% of the energy density in the universe is in the form of an unexplainable component with negative pressure, a property which we never observe in particle colliders and in earth-based lab experiments [83]. Also, the dark matter component is illusive in that it has not been observed in colliders yet, but nevertheless, seems to be the dominant component of non-relativistic matter and in fact significantly more abundant than the normal baryonic matter [83]. Instead of confirming the picture we have about how nature works, and enriching it with new details, the recent cosmological observations propounds a radically different picture [83]. This, although not expected, is not $a\ priori$ wrong or worrying, and we may just accept it as a result of observations [83].

However, if one is to accept this radically new view of how nature works, one would like to understand it both from the phenomenological and the fundamental point of view [83]. The problem is that we do not understand at a fundamental level why the, ΛCDM model should not be wrong [83]. We have not yet observed directly the particles which should compose dark matter [83]. More importantly, the observed value of the cosmological constant is very puzzling and not easy to understand [83]. It would then be reasonable to doubt the assumptions at the heart of the, ΛCDM model [83]. This could be because of misinterpretations of the observational data [83]. It is in fact possible that gravity may not be explained by, GR on very large scales or there exist new degrees of freedom (or even new laws of nature!) which show up only when we increase the length scales and the complexity of the system under study [83]. It may be that the $Copernican$ principle is not valid (which however, would be unsatisfactory from a philosophical point of view) [83]. If one or several of these things are valid, then the conclusion that, Λ is non-zero may be ill based [83]. It seems indeed worth exploring these other routes, before concluding that the view of the universe drawn by the, ΛCDM model is reliable [83].

The Cosmological Constant Problem

The history of the cosmological constant (CC) dates back from the first days of, GR and was introduced by $Einstein$ himself in order to obtain a static universe from his dynamical theory of spacetime [87]. After coming to the realization that such a universe was unstable [87], the, CC disappeared from the scene for several decades. However, it was realised that the, CC and vacuum energy give degenerate contributions to, EFE [70, 87]. A simple and direct calculation of the estimated value of the, CC contribution leads to the high value for the energy density of the, CC, $\rho \sim 10^{71} GeV^4$ [69, 72, 102, 109] which is obtained by combining the gravitational, $Planck$ and speed of light constants. If a, CC with such a high value was present in the early universe no structure could ever have been formed. To make such a large value compatible with the measured value of the, CC, $\rho \sim 10^{-47} GeV^4$, one has to consider that the, CC appearing in the, EFE fine tunes to the vacuum contribution to about 120 orders of magnitude [69, 72, 102, 109], unless some mechanism exists that sets to zero the vacuum contribution of quantum fields. It may be that a quantum theory of gravity will solve this issue but still the fine tuning problem remains to explain why the cosmological constant we observe is so small compared to all other energy scales of nature [69, 72, 102, 109]. The second problem with the, CC is the coincidence problem. In fact it is hard to explain why the, CC is comparable with that of, DM (dark matter) energy density at, $z \sim 1$ despite the different scaling of the energy densities and the fact that the, CC dominates for an infinite time in the future (check however [11] for an opposite point of view). The two scales are in principle not related and this second fine tuning problem can be rephrased as that of why the, CC is small enough to allow the formation of the large scale structures we observe. The third problem is that the, CC is unstable against quantum corrections. A given physical parameter is allowed to be small if it is protected by some symmetry. The, CC in, GR is not protected [100], and that is the biggest problem.

The dark energy (DE) models were introduced to solve these problems by providing a dynamic mechanism responsible for the observed accelerated expansion of the universe (see [3] for a thorough review) and by assuming that, Λ vanishes for some conjectured reason. This would imply that most, DE models cannot solve the, CC problem.

Backreaction and Dark Energy

If one wanted to describe the cosmological observations without adopting a non-zero cosmological constant, some of the hypothesis which underlie the, ΛCDM model have to be relaxed [83]. Despite the fact that all of them might not be correct, for simplicity we can study what happens

if we relax in turn just one of these assumptions, for example, the large scale homogeneity and isotropy assumption, the assumption that the universe is filled only with, CDM and standard model particles and the assumption that gravity is explained by, GR at all scales [83].

In spite of large scale isotropy being very well tested observationally, homogeneity is not [83]. It is usually assumed that we do not occupy a special place in the universe (the $Copernican$ principle), which implies homogeneity, but since this belongs to the realms of philosophy, it may be wrong after all [83]. In fact, if the Earth was situated near the center of a large, nearly spherical structure, the supernovae observations may be ascribed as due to the inhomogeneity, without having a non-zero, Λ [34, 93]. However, apart from being puzzling in the realms of philosophy, this situation poses another fine tuning problem, regarding the characteristic of the spherical structure and our position inside it [83]. Besides, it is not so comprehensible whether it is consistent with all the cosmological observations, not just supernova [57]. A different possibility is the fact that inhomogeneities may go non-linear triggering a sizeable effect on the evolution of the scale factor [83]. The time evolution does not decrease with the averaging procedure on the, EFE [83]. Therefore, the real scale factor that describes our universe is different from the one we get by solving the $Friedmann$ equations, and it may be that this difference is crucial in judging if, Λ is zero or not [83]: the universe may seem to accelerate at late times just because we do not take into account properly this effect. The influence of inhomogeneities on the evolution of the scale factor is called backreaction (check for example [33] and references in [57]): this would provide a dramatic resolution of the coincidence problem, because in this case the formation of structures and the apparent acceleration are correlated since they are both a consequence of the fact that inhomogeneities become non-linear [83]. However, there is no convincing demonstration that backreaction is indeed able to explain the secrets of apparent acceleration [83]. It should be noted anyway that it might significantly affect the approximations of cosmological parameters, even if it does not lead to acceleration [57].

Alternatively, if we take, $\Lambda = 0$, ignore backreaction and assume that large scale inhomogeneity and isotropy hold, we are forced to admit that either gravity is not explained exactly by, GR or that there are new degrees of freedom whose contribution to the energy-momentum tensor is responsible for the acceleration of the universe [83]. The scenario is somewhat similar to what happened when deviations from the predicted orbits were observed for some planets in the solar system [83]: in the case of anomalies of the orbits of $Uranus$ and, $Neptune$, the existence of a new, unobserved planet was predicted. $Pluto$ was later discovered [83]. On the other hand, the anomalous precession of the perihelion of mercury could not be explained as the effect of a yet unobserved object (originally called $Vulcan$) [83]: the discrepancy was shown to be due to the inadequacy of the $Newtonian$ theory of gravity, and the resolution of the problem was

the result of the development of a new theory of gravity, GR [83]. If we consider, GR to be the valid theory of gravity, even at extremely large scales, then the cosmological observations can be explained by adding a source term in the, EFE which by equation 1.35 would have to satisfy, $\rho + 3P < 0$ [83]. This is a very unusual property, because at the classical level the matter we observe in earth-based experiments have positive energy and non-negative pressure [83]. Therefore, not only do we need to introduce an ad-hoc matter which we do not observe on Earth and in the solar system, but this matter has to have very alien properties [83]. On the other hand, at quantum level such a property is not so unique, and can be possessed also by a very simple system such as a (classical) scalar field [83]. This new component of the energy-momentum tensor is usually termed dark energy (DE), and there are several different models or scenarios (such as for example quintessence models, K-essence and others, see [33]) which addresses the late time acceleration problem following this idea. However, most of them are not well motivated (so far) from the point of view of fundamental physics, and generally they do not solve the coincidence problem, since some type of fine tuning seems to be required anyway [57].

Lastly, we may assume that there is no, DE but observations just signal the breakdown of the validity of, GR at extremely large scales [83]. From this point of view, the explanation of the apparent acceleration is to be found in devising a new theory of gravity, which should reproduce very well the results of, GR on scales from a micron up to astrophysical scales [83]. This approach is usually termed modified gravity [83].

1.4 Thesis Outline

This thesis has been organised as follows:

In chapter 2 we give the $Lagrangians$ and relevant field equations for scalar-tensor theories of gravity, $Galileons$ and vector-tensor theories of gravity respectively. We also give reasons motivating these theories and discuss the viability of vector-tensor theories of gravity.

In chapter 3 we consider the case of the cosmological evolution in a particular vector-tensor theory of gravity with a potential and a $Galileon$-motivated interaction terms. The evolution of vector field self-interactions that are relatively related to $Galileon$ fields throughout the expansion history of the universe are considered and a classification of the parameters M and H according to the behaviour of the field in each cosmological epoch is carried out. We obtain an autonomous system for the inflationary case. The general features of the phasemaps are given and the critical point is appropriately characterised. It is not possible to obtain an autonomous system for radiation and

matter dominated epochs hence, we consider other analytical methods. We obtain eigenvalues and hence, phasemaps. The general features of the phasemaps are given and the point to which the trajectories on the phasemaps converge is appropriately characterised. We also give reasons motivating this particular theory of gravity.

Chapter 4 contains discussions on chapter 1, chapter 2, general final remarks on the work done in chapter 3, future work and concluding remarks on the work done in chapter 3.

Chapter 2. Modified Theories of Gravity

2.1 Introduction

In cosmology, the interest in modifying, GR has increased in recent years due to the existence of several problems which cannot be satisfactorily addressed within the framework of, GR without resorting to unknown matter components, namely, DM and, DE [47]. The need for new, DM particles first appeared so that the rotation curves of galaxies which indicate the existence of non-luminous matter in the haloes of such galaxies would be accounted for [47]. However, its presence is also very useful for the explanation of some cosmological observations. For instance, the formation and structures of galaxies and clusters [47].

The other dark component called Dark Energy (DE) is thought to be responsible for the accelerated expansion of the universe first inferred from observations of distant type Ia supernova [76] and subsequently confirmed by more precise supernovae measurements [56] as well as other cosmological probes, mainly, CMB temperature power spectrum and baryon acoustic oscillations (BAO) [85, 86, 88]. The accelerated expansion of the universe is explained by introducing a cosmological constant term in, EFE [47]. But this poses a problem from the theoretical point of view because its value, as observed, is extremely small compared to the natural scale of gravity set by $Newton's$ constant [47]. A theory with two scales differing in many orders of magnitude does not seem very $natural$, and for this, the problem is called the naturalness problem [47]. Therefore, many models trying to play the role of dynamical, DE models can be broadly classified in two classes [47]: on one hand, models in which, DE is a new field to add to the standard composition of the universe [103] and on the other, models in which the accelerated expansion would be an effect of a modified theory of gravity [17, 28]. However, this difference is not always very clear since some alternative gravity models require the introduction of new fields which, indeed, may play the role of, DE [47].

Attempts to renormalise, GR in the 1960s and 1970s showed clearly that counterterms should be introduced which changes the theory significantly and make its field equations be of fourth order instead of second [14]. From the point of view that is physical, this important truth implies that extra degrees of freedom, in addition to the usual spin two graviton, need to be introduced [14]. However, after corrections, the theory is not free from ghosts, which makes it non-unitary [14].

The corrections that are introduced by renormalisation are quadratic in the algebraic invariants of the curvature tensor [14].

The fourth reason why gravity should be modified is because of the shortcomings of the inflationary theory. The first order phase transition of a Grand Unified Theory (GUT) gave rise to the early models of inflation [38]. Despite these models leading to sufficient exponential expansion, completion of the transition through bubble percolation did not occur, and lack of bubble collisions meant that the interior of the bubbles was not reheated. Later models of inflation [2, 59] considered second-order transitions within the, GUT and hence, successfully ending inflation with reheating from oscillations of the scalar field. But the amplitude of relic density fluctuations predicted by these models is too high. This implies that, current models of inflation suggest second-order transitions in a completely new scalar field: the inflaton, Φ. The potential of this field, $V[\Phi]$ should have a very low gradient and curvature so that observed metric fluctuations are matched.

In inflation models of this type that are viable, reheated bubbles again typically do not percolate hence, inflation is $eternal$ and continues with exponential expansion in the region outside bubbles. These causally disconnected bubble universes constitute what is known as a $multiverse$ [15], where low-energy physics can vary between different bubbles.

The fifth reason why gravity should be modified is because of the so-called singularity problem [23, 39]. The cosmological singularity at time $t = 0$ is an infinite energy density state [39]. Therefore, this shows that, GR predicts its own breakdown [39].

One class of modified theories of gravity with an extra field are the so-called scalar-tensor theories of gravity (for example the $Brans - Dicke$ and $Horndeski$ theories of gravity). In the next section we will briefly consider these theories.

2.2 Scalar-Tensor Theories of Gravity

These theories of gravity are among some of the most (if not the most) established and well scrutinised modified theories of gravity [20]. They are usually utilised as the prototypical way in which deviations from, GR are modelled, and are of particular interest as their relatively less complicated structure of their field equations allow exact analytical solutions to be found in a number of physically interesting scenarios [20]. Scalar-tensor theories arise in a natural way as the dimensionally reduced effective theories of higher dimensional, such as $Kaluza - Klein$ and

string models [20]. They are also usually utilised as simple ways to self-consistently model possible variations in, G which is $Newton's$ constant [20].

2.2.1 Action and Field Equations

A general form of the scalar-tensor theory can be derived from the $Lagrange$ density [9], [66], [96]:

$$\mathcal{L} = \frac{1}{16\pi}\sqrt{-g}[f(\phi)R - g(\phi)\nabla_\mu\phi\nabla^\mu\phi - 2\lambda(\phi)] + \mathcal{L}_\mathcal{M}[\psi, h(\phi)g_{\mu\nu}], \tag{2.1}$$

where, f, g, h, λ are arbitrary functions of the scalar field, ϕ and, $\mathcal{L}_\mathcal{M}$ is the $Lagrangian$ density of the matter fields ψ. The functon $h(\phi)$ can be absorbed into the metric by a conformal transformation which is of the form [25]:

$$h(\phi)g_{\mu\nu} \to g_{\mu\nu}. \tag{2.2}$$

The conformal frame picked out by this option is one in which there is no direct interaction between the scalar field and matter fields, and is often taken to be the $Jordan$ frame [20]. Test-particles in this conformal frame follow geodesics of the metric to which they are coupled, and the weak equivalence principle is satisfied for massless test-particles [20]. The result of this transformation on the remainder of the $Lagrangian$ can then be absorbed into redefinitions of the as yet unspecified functions which are, f, g and, λ [20].

By redefining the scalar field ϕ we can fix, $f(\phi) \to \phi$, without losing generality [20]. The $Lagrangian$ density 2.1 can then be expressed as:

$$\mathcal{L} = \frac{1}{16\pi}\sqrt{-g}\left[\phi R - \frac{\omega(\phi)}{\phi}\nabla_\mu\phi\nabla^\mu\phi - 2\lambda(\phi)\right] + \mathcal{L}_\mathcal{M}[\psi, g_{\mu\nu}], \tag{2.3}$$

where, $\omega(\phi)$ is an arbitrary function, usually referred to as the $coupling\ parameter$, and, λ is a ϕ-dependent generalisation of the cosmological constant [20]. This theory reduces to the famous $Brans - Dicke$ theory [13] in the limit $\omega \to$ constant and $\lambda \to 0$, and approaches, GR with a cosmological constant in the limits $\omega \to \infty$, $\frac{\omega'}{\omega^2} \to 0$ and $\lambda \to$ constant.

The variation of the action obtained from integrating equation 2.3 over all space, with respect

to, $g^{\mu\nu}$, results in the field equations [20]:

$$8\pi T_{\mu\nu} \equiv \phi G_{\mu\nu} + \left[\Box\phi + \frac{1}{2}\frac{\omega}{\phi}(\nabla\phi)^2 + \lambda\right] g_{\mu\nu} - \nabla_\mu\nabla_\nu\phi - \frac{\omega}{\phi}\nabla_\mu\phi\nabla_\nu\phi. \tag{2.4}$$

Now, as well as the metric tensor $g_{\mu\nu}$, these theories also have the dynamical scalar field ϕ and therefore, we must vary the action obtained from equation 2.3 with respect to this additional degree of freedom [20]. After getting rid of, R with the trace of equation 2.4, this results in:

$$8\pi T = [2\omega + 3]\Box\phi + \omega'[\nabla\phi]^2 + 4\lambda - 2\phi\lambda', \tag{2.5}$$

where primes here symbolise differentiation with respect to, ϕ [20]. These are called the field equations of the theories of scalar-tensor gravity [20].

The other class of modified theories of gravity we will consider in the next section (and of particular interest to us) are the $Galileons$.

2.3 Galileons

$Galileon$ theory [64] was originally developed by $Nicolis\ et\ al.$ in order to facilitate a model independent analysis of a large class of alternative theories of gravity [20]. In all cases, GR on perturbed $Minkowski$ space is modified by adding an additional single scalar field, called the $Galileon$, with derivative self-interactions [20]. Despite both the $Galileon$ and the graviton coupling to matter, any direct coupling between them is negligible up to leading order [20]. The vacuum $Lagrangian$ that results does not change under the following shift in the $Galileon$ field [20]:

$$\pi \to \pi + b_\mu x^\mu + c. \tag{2.6}$$

This symmetry corresponds to a generalisation of $Galilean$ invariance and hence, the term given [20]. The model is inspired by $Dvali-Gabadadze-Porrati$ gravity (DGP) [28]. The $boundary\ effective\ theory$ on the, DGP is well explained by the action given below [20]:

$$S_{eff}^{DGP} = \int d^4x[\mathcal{L}_{\mathcal{GR}} + \mathcal{L}_\pi^{\mathcal{DGP}}], \tag{2.7}$$

where [20]:

$$\mathcal{L}_{\mathcal{GR}} = \frac{1}{16\pi G}\left[\frac{1}{4}\overline{h^{\mu\nu}}(\partial^2(\overline{h_{\mu\nu}} - \frac{1}{2}\overline{h}\eta_{\mu\nu}) + ...)\right] + \frac{1}{2}\overline{h_{\mu\nu}}T^{\mu\nu}, \tag{2.8}$$

$$\mathcal{L}_{\pi}^{\mathcal{DGP}} = \frac{1}{16\pi G}\left[\frac{1}{2}(3\pi\partial^2\pi - r_c^2(\partial\pi)^2\partial^2\pi)\right] + \frac{1}{2}\pi T. \tag{2.9}$$

It is easy to see that the action has two components [20]: a, GR piece that is linearised, and a modification that is due to the brane bending mode, $\mathcal{L}_{\pi}^{\mathcal{DGP}}$. All interactions go to zero in the decoupling limit except for the scalar self-interactions [20]. When $Nicolis\ et\ al.$ focused on the, π-$Lagrangian$, $\mathcal{L}_{\pi}^{\mathcal{DGP}}$ he observed that the vacuum field equations are built exclusively out of second derivatives, $\partial_\mu\partial_\nu\pi$ [20]. In particular, this implies that there are no terms that are higher than second order, and this ensues a well defined $Cauchy$ problem and also avoids any of the potential problems arising from ghosts in higher derivative theories [20]. Additionally, there are no first or zero derivative terms which implies that the, $\pi\ Lagrangians$ has the $Galilean$ symmetry [20]. This is as a result of $Poincare$ invariance in the bulk [68].

One would expect that almost any co-dimension one braneworld model with large distance deviations from, GR will be explained, in part, and in some appropriate limit, by a, $\pi\ Lagrangian$ that is generalised and has the $Galilean$ symmetry [20]. This essentially follows from the fact that the curvature of the brane that is extrinsic is given by, $K_{\mu\nu} \approx \partial_\mu\partial_\nu\pi$ on scales where the background curvature is negligible [20].

We should take note that even if there is no direct coupling to matter and henceforth, no alternative gravity, $Galileons$ are of interest in their own right as a source of energy-momentum [20]. Without even introducing any instability, one can particularly obtain violations of the null energy condition [24, 65]. Generally, however, a single $Galileon$ is said to result in superluminality, although the situation may be improved by considering the multi-$Galileon$ theory [20].

Finally, the class we will consider in the next section (and also of particular interest to us) are the vector-tensor theories of gravity.

2.4 Vector-Tensor Theories of Gravity

These theories have an extra field in addition to the metric tensor [47]. The gravitational action for these theories is modified by adding a vector field that is non-minimally coupled to gravity [47]. A primary reason for studying these theories is that they could be candidates for quantum gravity. A secondary aim is to come up with a viable and reasonably natural foil against which to compare gravitational observations [47]. The third reason is the theoretical laboratory it offers for studying diffeomorphism invariant physics with preferred frame effects. The study of vector-tensor theories to describe the gravitational interaction as modifications of, GR started a long time ago with the works by $Will$, $Nordtvedt$ and $Hellings$ [40] in the early $70s$ as candidates to produce preferred frame effects. These theories were then tested but the preferred frame effects were ruled out [47]. Therefore, the theories were abandoned [47]. Vector field fluctuations could be either timelike or spacelike so that those models were generally thought to present instabilities [47]. A detailed treatment on this problem was developed in [48] for the case without a potential term and in [4] for the case with a potential term and it was shown that there is still some room in the parameter space for stable models.

A special class of these theories re-emerged because of the increasing interest in models with $Lorentz$ violation [91]. The breaking of $Lorentz$ invariance was made possible by the presence of a vector field whose norm was to be constant by means of a $Lagrange$ multiplier [47]. Some of these models are even free of instabilities as it was shown in [48].

Quite recently, after the discovery of the accelerated expansion of the universe, vector-tensor theories supplemented without potential terms have much attention as possible candidates for, DE [45]. They have also been used for other cosmological purposes such as candidates to drive an inflationary epoch (although we still have the usual, CC problem) [50], to generate non-singular cosmologies [67], as, DM candidates [8], as sources of cosmological magnetic fields [81] and as candidates to solve some of the observed anomalies in the, CMB power spectrum [54].

2.4.1 Action and Field Equations

From the term $vector - tensor$, one can easily conclude that these theories involve the introduction of a space-time 4-vector field, A^{μ} [20]. A general action for these theories is expressed

as:

$$S = \int d^4x\sqrt{-g}\left[\frac{1}{16\pi G}R + \mathcal{L}(g^{\mu\nu}, A^\nu) + S_M(g^{\mu\nu}, \psi)\right], \tag{2.10}$$

where, S_M denotes the matter action [20]. We should take note that the matter fields ψ in, S_M couple only to the metric $g_{\mu\nu}$, and not to, A^ν [20]. A^μ has a time-like direction [20]. The simplest (and most thoroughly studied) type of these theories is quadratic in derivatives of, A^ν, and has the form:

$$\mathcal{L}_{\mathcal{EA}}[g^{\mu\nu}, A^\mu] = \frac{M^2}{16\pi G}F[K] + \frac{1}{16\pi G}[A^\mu A_\mu + 1], \tag{2.11}$$

where, $K^{\mu\nu}_{\alpha\beta} \equiv c_1 g^{\mu\nu}g_{\alpha\beta} + c_2\delta^\mu_\alpha\delta^\nu_\beta + c_3\delta^\mu_\beta\delta^\nu_\alpha - c_4 A^\mu A^\nu g_{\alpha\beta}$ [20]. The notation, $c_{12.....} = c_1 + c_2 + ...$ is used in what follows [20]. The theory derived from equations 2.10 and 2.11 is called the linear $Einstein$-aether theory [20].

A more general, non-linear $Lagrangian$ for the aether field can be expressed in the form:

$$\mathcal{L}_{\mathcal{GEA}}[g^{\mu\nu}, A^\mu] = \frac{M^2}{16\pi G}F[K] + \frac{1}{16\pi G}\lambda[A^\mu A_\mu + 1], \tag{2.12}$$

where, $K = K^{\mu\nu}_{\alpha\beta}\nabla_\mu A^\alpha \nabla_\nu A^\beta$, λ is the $Lagrange$ multiplier and, M has dimensions of mass [20]. This is called a generalised $Einstein$-aether theory [20].

Such an action appears from $Lorentz$ violating physics in quantum gravity [44]. Undoubtedly, the linear $Einstein$-aether theory can be constructed using the rules of effective field theory, and has been shown to be stable with regard to quantum effects [107]. However, such theories can suffer from instabilities at the classical level, with the onset of caustics in a finite time [22]. This raises the question of whether the vector field in these theories are just effective (possibly composite) degrees of freedom, or whether they could be genuine fundamental fields [20].

The field equations for this theory, obtained by varying the action for the generalised $Einstein$-aether theory with respect to, $g^{\mu\nu}$ are shown to be:

$$\begin{aligned} G_{\mu\nu} &= \tilde{T_{\mu\nu}} + 8\pi G T^{matter}_{\mu\nu}, \\ \tilde{T_{\mu\nu}} &= \frac{1}{2}\nabla_\alpha[F_K(J^\alpha_{(\mu}A_{\nu)} - J^\alpha_{(\mu}A_{\nu)} - J_{(\mu\nu)}A^\alpha)] \\ &- F_K Y_{(\mu\nu)} + \frac{1}{2}g_{\mu\nu}M^2F + \lambda A_\mu A_\nu, \end{aligned} \tag{2.13}$$

where, $F_K \equiv \frac{dF}{dK}$ and, $J^\mu_\alpha \equiv [K^{\mu\nu}_{\alpha\beta} + K^{\nu\mu}_{\beta\alpha}]\nabla_\nu A^\beta$ [20]. Brackets around indices symbolise symmetri-

sation, and, $Y_{\mu\nu}$ is defined by the functional derivative which is given by, $Y_{\mu\nu} = \nabla_\alpha A^\rho \nabla_\beta A^\sigma \frac{\partial [K^{\alpha\beta}_{\rho\sigma}]}{\partial g^{\mu\nu}}$ [20]. The equations of motion we can obtain for the vector field after varying with respect to, A^ν are:

$$\nabla_\mu [F_K J^\mu_\nu] + F_K y_\nu \;\; = \;\; 2\lambda A_\nu, \tag{2.14}$$

where we have taken the liberty to define, $y_\nu = \nabla_\alpha A^\rho \nabla_\beta A^\sigma \frac{\partial [K^{\alpha\beta}_{\rho\sigma}]}{\partial A^\nu}$ [20]. Lastly, in order to fix, $A^\nu A_\nu = -1$ the action is varied with respect to, λ [20].

In the next subsection we will consider a brief summary of the viability of vector-tensor theories of gravity.

2.4.2 Viability of Vector-Tensor Theories of Gravity

After some initial proposals, these theories were practically forgotten as mentioned earlier due to consistency problems and only particular classes of models with fixed norm vector or potential terms have been tackled in the context of violations of $Lorentz$ invariance (see [12] and references therein). However, very recently, it was shown in [45], [46] as mentioned earlier that unconstrained vector-tensor theories without potential terms are excellent candidates for, DE.

The three main problems found in these type of theories were the following [32, 35]:

a) Inconsistencies with local gravity tests: in addition to modifications in the static parametrised post-$Newtonian$ (PPN) parameters $[\gamma, \beta]$ (these parameters are a set of quantities that characterise most of gravity theories at small scales) [47], these theories usually predict preferred frame effects, parametrised by $[\alpha_1, \alpha_2]$. γ determines how much of space curvature g_{ij} is produced by a unit rest mass [31, 105], β determines how much nonlinearity is there in the law of superposition for gravity g_{00} [105] and α_1 or α_2 measure the strength and specific manner in which motion in the preferred frame affects the post-$Newtonian$ metric [105].

b) Classical instabilities: they are created by the presence of modes with negative propagation speed squared. Examples are: i) tachyonic instabilities [7]: hypothetical particles which travel faster than the speed of light are historically called tachyons [75]. Since the relativistic relation, $v = \frac{P}{\sqrt{P^2+m^2}}$ between velocity v and momentum P clearly gives, $v \leq 1$ unless mass-squared $m^2 < 0$, tachyons would carry negative, m^2 [7]. From a more modern perspective, the term $tachyon$ is recycled to refer to a quantum field with, $m^2 \equiv V'' < 0$ where, V is the potential and double prime refers to second-order differentiation [7]. The idea of faster-than-light propagation

is abandoned [7]. Clearly, one can see that, V'' can be negative about a maximum of the potential [7]. Since the dynamics of the system will tend to minimise the energy, fluctuations about such a point will be unstable [7]. Therefore, tachyons are then associated with the presence of some physical instability [7]. These instabilities are admissible. Tachyons also play a role in the breaking of symmetry and the formation of cosmic defects [7]. ii) $Laplacian$ instabilities: $Gauss's$ law explains that the divergence of any electric force field possible is zero in free space. An electrical force $F[\overline{r}]$ deriving from a potential $V[\overline{r}]$ in mathematical notation will always be divergenceless (and hence, satisfy $Laplace's$ equation): $\nabla.\overline{F} = -\nabla^2 V = 0$. This implies that there are no local minima or maxima of the field potential in free space, only saddle points. Hence, there cannot be a particle of stable equilibrium. Therefore, at least in one direction, there must be an instability. This instability is called a $Laplacian$ instability but it is not admissible.

c) Quantum instabilities (ghosts): they usually appear when the energy of perturbation modes become negative.

The viability of any extended theory of gravity is subject to its agreement with solar system experiments, which provide very tight constraints on the, PPN parameters [47]. For a general vector-tensor theory, it was shown that there are neither preferred location effects nor violation of total momentum conservation [47]. However, these theories usually lead to preferred frame effects (as expected due to the presence of a vector field) as well as deviations from, GR for the static, PPN parameters [47]. One can obtain constraints on the vector field from current observational limits on the, PPN parameters by linearising the parameters [47]. Hence, it was found that, typically, the vector field on the solar system scales will be constrained to be, $10^{-2} \gtrsim A$ for models in which all parameters are order unity and, A is the value of the vector field at solar system scales (in units of $4\pi G$) [47]. This value of the vector field does not need to coincide with its cosmological value [47].

Although a general vector-tensor theory will be constrained by the limits mentioned above, there are a number of models whose parameters satisfy certain relations, so that some of the, PPN parameters could be identical to those of, GR [47]. It was shown in [48] that there exist a total of 6 models which are indistinguishable from, GR by means of local gravity tests for any value of the background vector field.

The propagation speeds of scalar, vector and tensor perturbations were also studied and conditions for classical stability of the 6 models were obtained [48]. The energy density of the different modes were calculated and conditions for the absence of ghosts in the quantum theory were found [48]. It was found that only theories of the $Maxwell$ type or $Maxwell$ plus a gauge-fixing term can be made compatible with all the consistency conditions for arbitrary, A [48]. It was shown in [46]

that the electromagnetic theory with gauge fixing term can explain in a natural way the existence and the smallness of the cosmological constant, solving in this way the problem of establishing what is the fundamental nature of, DE.

With the increasing interest in vector-tensor theories of gravity in order to understand the wide variety of cosmological problems, it would seem useful to consider more general vector field self-interactions that can give interesting phenomenologies for the cosmological evolution and that are relatively related to $Galileon$ fields. Therefore, we consequently perform this so that one can determine whether this particular theory is able to play a determined role in the history of the universe. In the next chapter, we focus on this issue.

Chapter 3. Vector-Galileon-Tensor Theories of Gravity

3.1 Introduction

As mentioned in the previous chapter, on the increasing interest of vector-tensor theories of gravity in order to understand the wide variety of cosmological problems, we will then consider more general vector field self-interactions that can give interesting phenomenologies for the cosmological evolution and that are relatively related to $Galileon$ fields. Therefore, in this chapter we will explore the theory with a potential term, $V[A^2] = \frac{1}{2}M^2A^2$ and a $Galileon$-motivated interaction term, $G[A^2] = \lambda A^2$. M is the mass term, λ is a dimensionless parameter and, $A^2 = A_\mu A^\mu$ for a vector field, A_μ.

Therefore, we start by writing an action for a vector-$Galileon$-tensor theory:

$$S[g_{\mu\nu}, A_\mu] \;=\; \int d^4x\sqrt{-g}\bigg[-\frac{1}{16\pi G}R - \frac{1}{4}F_{\mu\nu}F^{\mu\nu} + \frac{1}{2}M^2A^2 + \lambda A^2\nabla_\mu A^\mu\bigg], \qquad (3.1)$$

where, $F_{\mu\nu} = \partial_\mu A_\nu - \partial_\nu A_\mu$, the third term is the potential term, the coefficient of, $\nabla_\mu A^\mu$ in the fourth term is the $Galileon$ term and for subsequent calculations, we will use this action first.

A set of field equations for, A_μ can be obtained by varying the action with respect to the vector field to give:

$$\nabla_\mu F^{\mu\nu} + [M^2 + 2\lambda\nabla_\mu A^\mu]A^\nu - \lambda\nabla^\nu A_\mu A^\mu \;=\; 0. \qquad (3.2)$$

Since the interest is in the cosmological evolution of vector field self-interactions that are relatively related to $Galileon$ fields on a, $FLRW$ background, it is assumed that the field does not affect the background metric meaning that it will be treated as a test field and also assumed to be homogeneous. The spatial component of the field lying along the, z-axis is chosen in such a way that, $A_\mu = [A_0(t), 0, 0, A_z(t)]$. This form of the field assumes linear polarisation. When the field

oscillates, other types of polarisations are avoided. The metric is taken to be:

$$ds^2 = dt^2 - a(t)^2[dx^2 + dy^2 + dz^2], \tag{3.3}$$

where, a is the scale factor. For this metric, the field equations read:

$$2\lambda A_z \dot{A}_z + a^2 M^2 A_0 + 6\lambda H a^2 A_0^2 = 2\lambda H A_z^2, \tag{3.4}$$

$$\begin{aligned} 0 &= -\frac{1}{6a^3H^2}\Bigg[3M^2A_z aH^2 + 6\ddot{A}_z aH^2 + A_z M^2 \dot{H} a + 6\dot{A}_z H^3 a \\ &- \frac{1}{\sqrt{M^4a^2 - 48\lambda^2 H A_z \dot{A}_z + 48\lambda^2 H^2 A_z^2}}\Big(48A_z^2H^3\lambda^2\dot{A}_z - 3A_z M^4 a^2 H^2 + 24A_z\lambda^2\dot{A}_z^2 H^2 \\ &+ 24A_z^2\lambda^2\ddot{A}_z H^2 - 24A_z^2\lambda^2\dot{H}\dot{A}_z H - 96A_z^3H^4\lambda^2 + A_z\dot{H}M^4a^2\Big)\Bigg], \end{aligned} \tag{3.5}$$

where a dot stands for a derivative with respect to the cosmic time t and, $H = \frac{\dot{a}}{a}$ is the expansion rate. One can introduce a more relatively physical variable, $B_z = \frac{2\lambda A_z}{a}$. With this, one can rewrite equation 3.4 in a more useful form as:

$$A_0 = -\frac{M^2 + \epsilon\sqrt{M^4 - 12B_z\dot{B}_z H}}{24\lambda^2 H}, \tag{3.6}$$

and it is composed of two branches of solutions. $\epsilon = \pm 1$ parametrises the two branches of solutions. We can rewrite equation 3.4 as:

$$\dot{A}_z = \frac{2\lambda H A_z^2 - a^2 M^2 A_0 - 6\lambda H a^2 A_0^2}{2\lambda A_z}, \tag{3.7}$$

or:

$$A_z = \frac{2\lambda\dot{A}_z + \epsilon\sqrt{4\lambda^2\dot{A}_z^2 + 8\lambda H a^2 A_0[M^2 + 6\lambda H A_0]}}{4\lambda H}. \tag{3.8}$$

3.8 has two branches of solutions. $\epsilon = \pm 1$ parametrises both branches of solutions. We insert equation 3.7 or 3.8 into equation 3.5. After that, we then insert equation 3.6, $\frac{\dot{a}}{a} = H$ and,

$A_z = \frac{aB_z}{2\lambda}$ into the resulting equation. We obtain (valid for a power law, $a \propto t^p$):

$$\begin{aligned} 0 &= \left[\epsilon\frac{B_z^2}{M^2} + \sqrt{1-X}\right]\ddot{B}_z + 3H\left[\frac{\epsilon M^2}{36H^2}X + \sqrt{1-X}\right]\dot{B}_z - M^2\frac{\epsilon}{2}\left[1+\frac{1}{3p}\right]B_z \\ &+ M^2\left[\frac{\epsilon}{2}\left(1+\frac{1}{6p}\right)X + \left(\frac{1}{2}\left(\frac{1}{3p}-1\right) + \frac{H^2}{M^2}\left(\frac{1}{p}-2\right)\right)\sqrt{1-X}\right]B_z, \end{aligned} \tag{3.9}$$

where, $X = \frac{12B_z\dot{B}_z H}{M^4}$ and, $p = -\frac{H^2}{\dot{H}}$ (p is not to be mistaken for pressure). For the small field limit ($X \ll 1$) where, $\sqrt{1-X} \simeq 1 - \frac{1}{2}X + O(X^2)$, equation 3.9 reduces to:

$$\begin{aligned} 0 &= \left[1 + \epsilon\frac{B_z^2}{M^2} - \frac{6B_z\dot{B}_z H}{M^4}\right]\ddot{B}_z + 3H\left[\epsilon\frac{M^2}{36H^2}X + 1 - \frac{6B_z\dot{B}_z H}{M^4}\right]\dot{B}_z \\ &- M^2\left[\frac{\epsilon}{2}\left(1+\frac{1}{3p}\right) + \frac{1}{2}\left(\frac{1}{3p}-1\right) + \frac{H^2}{M^2}\left(\frac{1}{p}-2\right)\right]B_z \\ &+ M^2\left[\left(-\frac{1}{4}\left(\frac{1}{3p}-1\right) - \frac{H^2}{2M^2}\left(\frac{1}{p}-2\right) - \frac{\epsilon}{2}\left(1+\frac{1}{6p}\right)\right)X\right]B_z, \end{aligned} \tag{3.10}$$

where the effective mass initially is:

$$m_{eff}^2 = -M^2\left[\frac{\epsilon}{2}\left(1+\frac{1}{3p}\right) + \frac{1}{2}\left(\frac{1}{3p}-1\right) + \frac{H^2}{M^2}\left(\frac{1}{p}-2\right)\right], \tag{3.11}$$

for, $X \ll 1$ and, $\frac{H^2X}{M^2} \ll 1$. If, $H^2 \ll M^2$, the effective mass in equation 3.11, reduces to:

$$m_{eff0}^2 = -M^2\left[\frac{\epsilon}{2}\left(1+\frac{1}{3p}\right) + \frac{1}{2}\left(\frac{1}{3p}-1\right)\right], \tag{3.12}$$

while when, $\frac{H^2}{M^2} \gg 1$ and, $p \neq \frac{1}{2}$, it is:

$$m_{eff1}^2 = -H^2\left[\frac{1}{p}-2\right]. \tag{3.13}$$

The friction term in equation 3.10 is:

$$friction - term = 3H\left[\frac{\epsilon M^2}{36H^2}X + 1 - \frac{6B_z\dot{B}_z H}{M^4}\right]. \tag{3.14}$$

The competing terms are, $\frac{\epsilon M^2}{36H^2}X$ and 1. Assuming that, $\frac{M^2}{36H^2}X \ll 1$, the friction term reduces

to:

$$friction - term_0 \;=\; 3H\left[1 - \frac{6B_z\dot{B}_z H}{M^4}\right]. \tag{3.15}$$

We want to study the evolution of vector field self-interactions that are relatively related to $Galileon$ fields in the different epochs (that is the inflationary epoch, radiation dominated epoch and matter dominated epoch) of the expansion history of the universe for the different cases, $H^2 \ll M^2$ and, $\frac{H^2}{M^2} \gg 1$.

We will first consider the case, $M^2 \ll H^2$. Assuming that, $B^2 \ll M^2$, considering equations 3.13 and 3.15, equation 3.10 reduces to:

$$\ddot{B}_z + 3H\dot{B}_z - H^2\left[\frac{1}{p} - 2\right]B_z \;=\; 0, \tag{3.16}$$

where the effective mass is $m^2_{eff2} = \left[2 - \frac{1}{p}\right]H^2$ and the friction term is $3H$. If, $m^2_{eff2} > 0$ we expect the field to oscillate while if, $m^2_{eff2} < 0$ we expect the field to grow exponentially. But if, $m^2_{eff2} \gg 3H$, then we can approximate equation 3.16 to:

$$\ddot{B}_z + \left[2 - \frac{1}{p}\right]H^2 B_z \;=\; 0, \tag{3.17}$$

whose solution is given by:

$$B_z \sim \exp\left[\int \sqrt{-\left(2 - \frac{1}{p}\right)H^2 dt}\right]. \tag{3.18}$$

Thus, if, $\left[2 - \frac{1}{P}\right]H^2 > 0$, we have, $H\sqrt{\frac{1}{p} - 2}$ as imaginary and the solution will oscillate. The term, $3H$ will affect the amplitude of the oscillations. The general solution is then given by:

$$B_z \sim \frac{1}{\sqrt{3H}}\exp\left[\int \sqrt{-\left(2 - \frac{1}{p}\right)H^2 dt}\right]. \tag{3.19}$$

But if, $\left[2 - \frac{1}{p}\right]H^2 < 0$, $H\sqrt{\frac{1}{p} - 2} \in \mathbb{R}$, we expect the field to have an exponential behaviour.

If, $m^2_{eff2} \ll 3H$ where, $m^2_{eff2} > 0$, then we can approximate equation 3.16 to:

$$\ddot{B}_z + 3H\dot{B}_z = 0, \tag{3.20}$$

whose solution is given by:

$$\dot{B}_z \sim \exp\left[-\int 3H dt\right], \tag{3.21}$$

which is the amplitude of oscillations. The term, $3H$ affects the amplitude of oscillations or, $\dot{B}_z$.

We then solve the full equation 3.9 numerically and compare with the analytical predictions to see if they match.

Let us now consider the case, $M^2 \gg H^2$. Assuming that, $B^2 \ll M^2$, using equations 3.12 and 3.15, equation 3.10 reduces to:

$$\ddot{B}_z + 3H\dot{B}_z - M^2\left[\frac{\epsilon}{2}\left(1+\frac{1}{3p}\right)+\frac{1}{2}\left(\frac{1}{3p}-1\right)\right]B_z = 0, \tag{3.22}$$

where the effective mass is $m^2_{eff3} = M^2\left[\frac{1}{2}\left(1-\frac{1}{3p}\right)-\frac{\epsilon}{2}\left(1+\frac{1}{3p}\right)\right]$ and the friction term is $3H$. If, $m^2_{eff3} > 0$ we expect the field to oscillate while if, $m^2_{eff3} < 0$ we expect the field to grow exponentially. But if, $m^2_{eff3} \gg 3H$, then we can approximate equation 3.22 to:

$$\ddot{B}_z + M^2\left[\frac{1}{2}\left(1-\frac{1}{3p}\right)-\frac{\epsilon}{2}\left(1+\frac{1}{3p}\right)\right]B_z = 0, \tag{3.23}$$

whose solution is given by:

$$B_z \sim \exp\left[\int \sqrt{-M^2\left(\frac{1}{2}\left(1-\frac{1}{3p}\right)-\frac{\epsilon}{2}\left(1+\frac{1}{3p}\right)\right)}\,dt\right]. \tag{3.24}$$

Thus, if, $M^2\left[\frac{1}{2}\left(1-\frac{1}{3p}\right)-\frac{\epsilon}{2}\left(1+\frac{1}{3p}\right)\right] > 0$, we have, $M\sqrt{\frac{\epsilon}{2}\left[1+\frac{1}{3p}\right]+\frac{1}{2}\left[\frac{1}{3p}-1\right]}$ as imaginary and the solution will oscillate. The term, $3H$ will affect the amplitude of the oscillations. The

general solution is given by:

$$B_z \sim \frac{1}{\sqrt{3H}} \exp\left[\int \sqrt{-M^2\left(\frac{1}{2}\left(1-\frac{1}{3p}\right)-\frac{\epsilon}{2}\left(1+\frac{1}{3p}\right)\right)}dt\right]. \tag{3.25}$$

But if, $M^2\left[\frac{1}{2}\left(1-\frac{1}{3p}\right)-\frac{\epsilon}{2}\left(1+\frac{1}{3p}\right)\right] < 0$, $M\sqrt{\frac{\epsilon}{2}\left[1+\frac{1}{3p}\right]+\frac{1}{2}\left[\frac{1}{3p}-1\right]} \in \mathbb{R}$, the field will have an exponential behaviour. This is explained clearly in appendix A. But if, $m^2_{eff3} \ll 3H$ where, $m^2_{eff3} > 0$, then we can approximate equation 3.22 to 3.20 whose solution is given by equation 3.21, which is the amplitude of oscillations. The term, $3H$ affects the amplitude of oscillations or, $\dot{B}_z$. This is explained clearly in appendix A.

We then solve the full equation 3.9 numerically and compare with the analytical predictions to see if they match.

Therefore, in the next sections, a study of the evolution of vector field self-interactions that are relatively related to $Galileon$ fields in the different epochs (inflationary epoch, radiation dominated epoch and matter dominated epoch) of the expansion history of the universe for the different cases, $H^2 \ll M^2$ and, $\frac{H^2}{M^2} \gg 1$ is carried out. We also use the two-dimensional dynamical systems approach to analyse the system during the inflationary epoch. Although no autonomous equations are found for the interesting epochs of radiation or matter domination, other analytical methods are used to try and grapple with the dynamics.

3.2 Inflationary Epoch

3.2.1 Inflationary Epoch for the Cases, $M^2 \gg H^2$ and, $M^2 \ll H^2$

During the era of inflation, the universe undergoes an exponential expansion so that the $Hubble$ parameter H is a constant which implies that, $a \propto \exp(Ht)$. This corresponds to, $p \to \infty$.

We first consider the case where, $M^2 \ll H^2$. It can be seen that equation 3.16 reduces to:

$$\ddot{B}_z + 3H\dot{B}_z + 2H^2 B_z = 0, \tag{3.26}$$

where the effective mass is $m^2_{eff} = 2H^2$. For this epoch, the friction term 3.14 also reduces to $3H$ for the conditions, $B_z^2 \ll M^2$ and, $M^2 \lesssim H^2$. For radiation and matter epochs, the

condition, $M^2 \lesssim H^2$ is violated as, H which is time t dependent, decreases. The solution to equation 3.26 is:

$$B_z \;=\; c_1 \exp[-2Ht] + c_2 \exp[-Ht], \tag{3.27}$$

where, c_1 and, c_2 are constants.

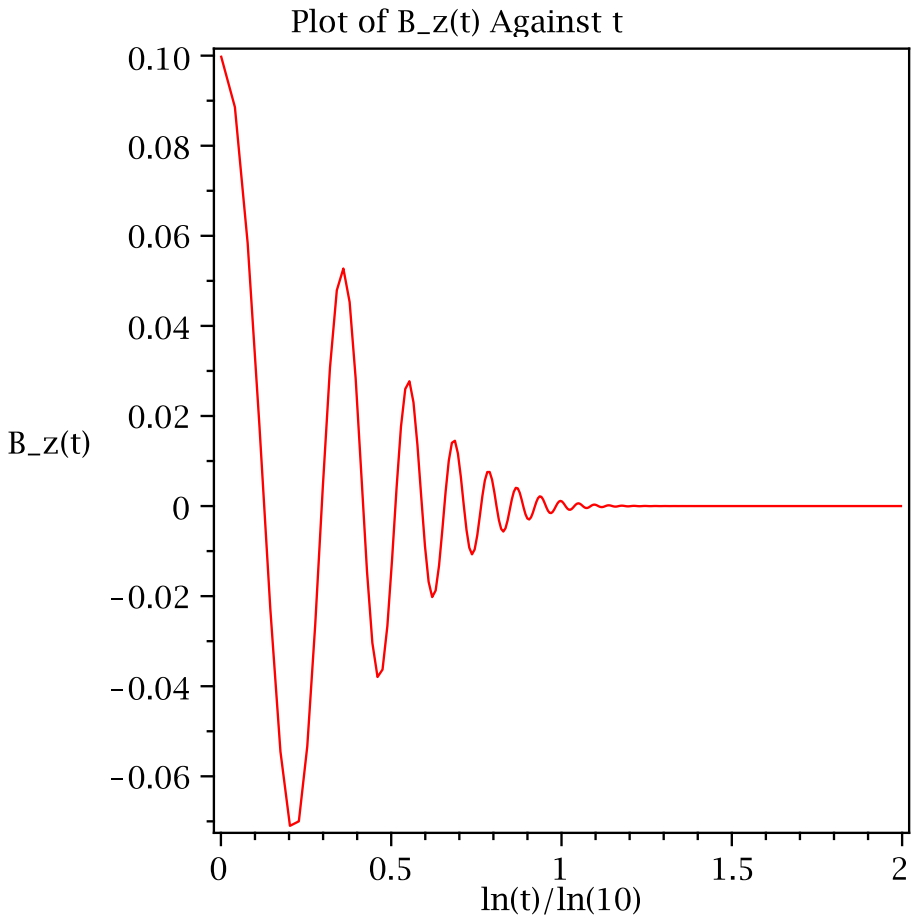

Figure 3.1: Field oscillations decaying by a factor, $a^{-\frac{1}{2}}$ until it is completely damped out. The case we consider for this plot is, $M^2 \ll H^2$. The values we use for, M and, H are 10^{-5} and 1 respectively. The time t is in the range $1 \leq t \leq 100$. The initial values for, B..z(t)=B_z and, $\dot{B}_z$ we use are $\exp[-1]$ and 0 respectively.

Since, $m_{eff}^2 > 0$, the field is expected to oscillate and from the friction term $3H > 0$ one expects the amplitude of the oscillations to decay with time t. This is explained in appendix A.

The full equation 3.9 when, $p \to \infty$ is expressed as:

$$\begin{aligned} 0 &= \left[\frac{\epsilon B_z^2}{M^2} + \sqrt{1-X}\right]\ddot{B}_z + 3H\left[\frac{\epsilon M^2}{36H^2}X + \sqrt{1-X}\right]\dot{B}_z \\ &- M^2\left[\frac{\epsilon}{2} - \frac{\epsilon X}{2} - \left(\frac{1}{2} + \frac{2H^2}{M^2}\right)\sqrt{1-X}\right]B_z. \end{aligned} \tag{3.28}$$

We then solve it numerically. For the values of, M and, H which are 10^{-5} and 1 (these values satisfy the case, $M^2 \ll H^2$) respectively, the field oscillates as expected. The amplitude decays as expected by a factor of, $a^{-\frac{1}{2}}$. This is shown in figure 3.1.

The next possibility that needs to be considered is, $M^2 \gg H^2$.

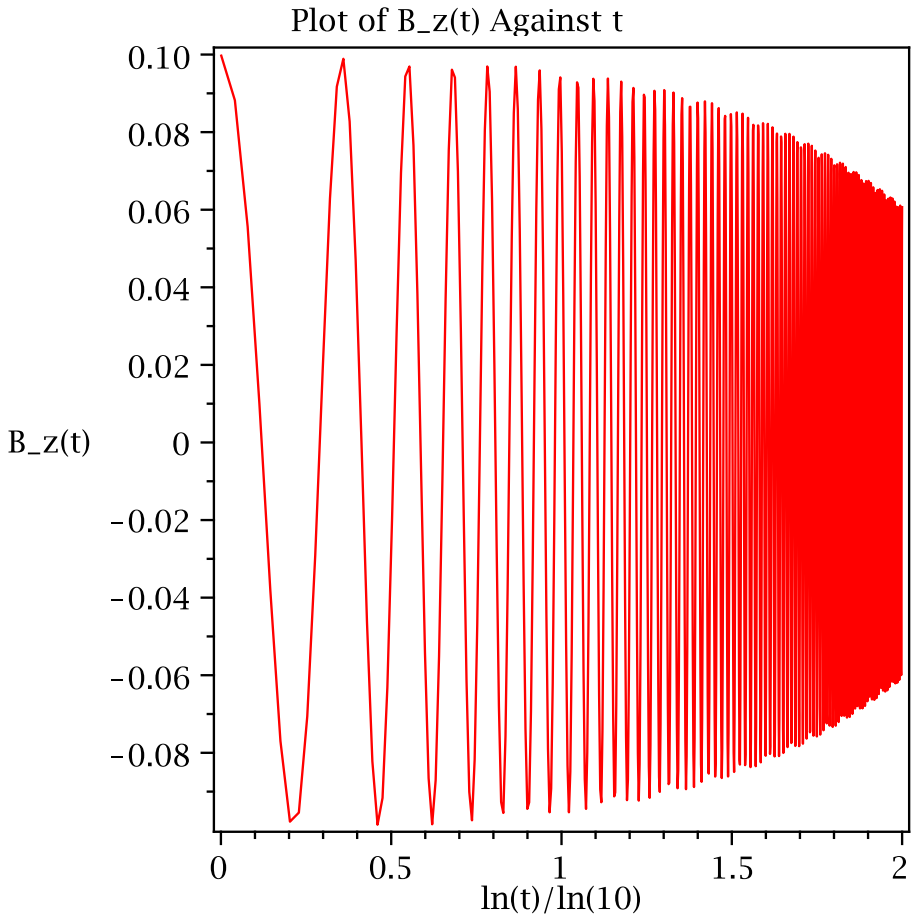

Figure 3.2: Field oscillations decaying by a factor, $a^{-\frac{1}{2}}$. The case we consider for this plot is, $M^2 \gg H^2$. The values we use for, M and, H are 1 and 10^{-2} respectively. Time t is in the range $1 \leq t \leq 100$. The initial values for, B..z(t)=B_z and, $\dot{B}_z$ we use are $\exp[-1]$ and 0 respectively.

Using, $\epsilon = -1$ it can be seen that equation 3.22 reduces to:

$$\ddot{B}_z + 3H\dot{B}_z + M^2 B_z = 0. \tag{3.29}$$

The solution to equation 3.29 is:

$$B_z = \exp\left[-\left(\frac{3H}{2}t\right)\right][c_1 \cos\omega t + c_2 \sin\omega t], \tag{3.30}$$

where, c_1 and, c_2 are constants as shown in appendix C. M^2 is the effective mass and, $3H$ is the friction term. Since, $M^2 \gg 3H$, equation 3.29 can be approximated to:

$$\ddot{B}_z + M^2 B_z = 0, \tag{3.31}$$

which has a solution given by:

$$B_z \sim \exp\left[\int \sqrt{-M^2}dt\right]. \tag{3.32}$$

$M^2 > 0$, and so, $\sqrt{-M^2}$ is imaginary hence, the solution oscillates. But from, $3H > 0$ in equation 3.29 one expects the amplitude of oscillations to decay with time t. The general solution is:

$$B_z \sim \frac{1}{\sqrt{3H}} \exp\left[\int \sqrt{-M^2}dt\right]. \tag{3.33}$$

This is explained in appendix A.

We then solve the full equation 3.28 numerically. For the values of, H and, M which are 10^{-2} and 1 (these values satisfy the case, $M^2 \gg H^2$) respectively, the field oscillates as expected. The amplitude decays as expected by a factor of, $a^{-\frac{1}{2}}$. This is shown in figure 3.2. This is explained in appendix A.

Endnote

For the cases, $M^2 \gg H^2$ and, $M^2 \ll H^2$ during the inflationary epoch, we can see some of the interesting phenomenologies for the evolution of vector field self-interactions that are relatively related to $Galileon$ fields. The field oscillates with decaying amplitude.

3.2.2 Dynamical Systems Analysis for Inflationary Epoch

A detailed treatment of two-dimensional dynamical systems is given in appendix B. In this subsection, we apply this approach during the inflationary epoch. This allows us to consider the full equation 3.28. Our aim is to obtain critical points and then study the evolution of small perturbations around them to see if the solution, B_z is stable or not.

For the subsequent analysis, it would be convenient to introduce, $x = B_z$ and, $y = \dot{B}_z$ so that we obtain the following autonomous system (as in equation 2.2 of appendix B):

$$\begin{aligned} \dot{x} &= y, \\ 0 &= \left[\frac{\epsilon x^2}{M^2} + \sqrt{1-X}\right]\dot{y} + 3H\left[\frac{\epsilon M^2}{36H^2}X + \sqrt{1-X}\right]y \\ &- M^2\left[\frac{\epsilon}{2}(1-X) - \left(\frac{1}{2} + \frac{2H^2}{M^2}\right)\sqrt{1-X}\right]x. \end{aligned} \tag{3.34}$$

These two equations can be combined leading to the following equation for the trajectories in the phasemaps we expect:

$$\begin{aligned} 0 &= \left[\frac{\epsilon x^2}{M^2} + \sqrt{1-X}\right]\frac{dy}{dx} - M^2\left[\frac{\epsilon}{2}(1-X) - \frac{1}{2}\sqrt{1-X}\right]\frac{x}{y} \\ &+ M^2\left[\frac{2H^2}{M^2}\sqrt{1-X}\right]\frac{x}{y} + 3H\left[\frac{\epsilon M^2}{36H^2}X + \sqrt{1-X}\right]. \end{aligned} \tag{3.35}$$

This equation can be integrated if values are given for the parameters, M and, H, although we shall not do it. However, we shall study the phasemaps and, from their features, we shall obtain the relevant information.

In equations 3.34 we see that the equation, $\dot{x} = 0$ has one solution: $B_z = 0$ and hence: in equations 3.34 again the solutions of, $\dot{y} = 0$ are, $\frac{\epsilon B_z^2}{M^2} + \sqrt{1-X} = 0$ (separatrix), $1 - X = 0$ (this is a curve for the boundary of the physical and non-physical regions), $1 - X < 0$ (non-physical region) and, $\dot{B}_z = 0$. This means that, the autonomous system has generally one critical point: $P_0 = (0, 0)$.

The separatrix above is obtained after obtaining the curve along which the coefficient of, $\dot{y}$ vanishes or, after making, $\dot{y}$ of the system 3.34 the subject of the formula, the denominator in the differential equation vanishes so that the equations are singular and therefore, trajectories cannot pass or go through it. Hence, we expect a separatrix on the phasemap or phasemaps.

The separatrix we expect should be a curve. We expect a non-physical region on the phasemap or phasemaps because of the square-root sign in the system 3.34. The separatrix should be inside the physical region or at the boundary of the physical and non-physical regions.

A critical point (or critical state) is the end point of a phase space. Near a critical point, all modes of behaviour of trajectories become similar or different modes of behaviour of the trajectories originally turn out to be identical from one another. For this reason, we then study the evolution of small perturbations around the critical point to see if the solution, B_z or, x is stable or not. With the presence of the separatrix, the non-physical region and the critical point P_0 we expect the trajectories to end in the critical point or in the limit of the not allowed region or the non-physical region. We want to find out if, P_0 is always stable or an attractor irrespective of the values of the parameters, H and, M.

To study the stability of the critical point P_0 we first linearise equation 3.34 around, P_0 then we find eigenvalues as illustrated in appendix B section $B.2$. We find that there are two sets of eigenvalues. This is so because, ϵ parametrises the two branches of equation 3.34. From the two sets of eigenvalues, we can determine what features to expect on the phasemaps. After obtaining the phasemaps, we study the trajectories near the critical point to see if, P_0 is stable or not or if the stability of, P_0 matches the analytical predictions.

As mentioned above we can study the particular features of the critical point P_0 according to the values and conditions of the parameters H and M:

- $P_0 = (0, 0)$. The eigenvalues of the linearised system of 3.34 around the critical point P_0 are:

$$[-2H, -H], \left[\frac{1}{2}(-3H - \sqrt{H^2 - 4M^2}), \frac{1}{2}(-3H + \sqrt{H^2 - 4M^2})\right], \tag{3.36}$$

  where, $[-2H, -H]$ is the first and, $\left[\frac{1}{2}(-3H - \sqrt{H^2 - 4M^2}), \frac{1}{2}(-3H + \sqrt{H^2 - 4M^2})\right]$ is the second set of eigenvalues. Thus, we have that the critical point is locally asymptotically stable for the first set of eigenvalues since all the eigenvalues are negative (according to theorem $B.2.1$ of appendix B). Trajectories of a dynamical system are continous and not self intersecting, though not generally closed. For this set of eigenvalues, the dynamical system is hyperbolic. Every orbit of the system is attracted to the origin (0,0) asymptotically. This means that all trajectories converge to the critical point as time $t \to \infty$. Hence, the critical point is an attractor or sink. This is explained clearly in theorem $B.2.1$

of appendix B.

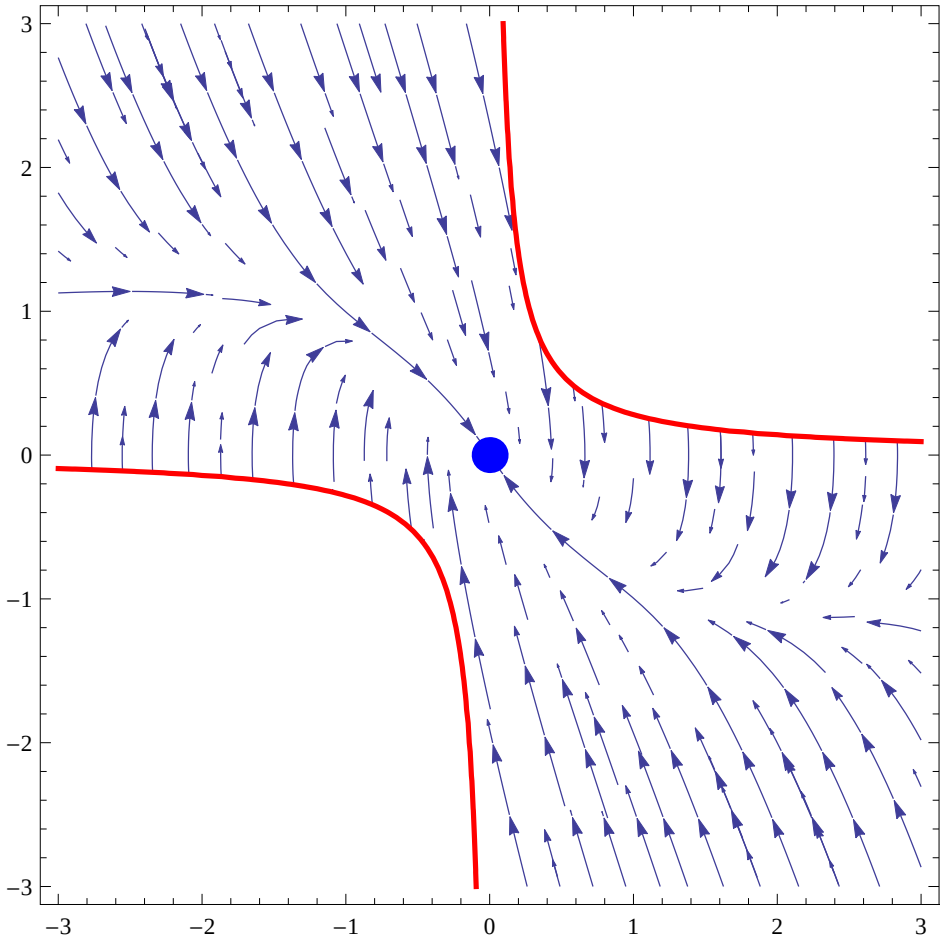

Figure 3.3: The first set of eigenvalues, $[-2H, -H]$, is considered for this plot. All the trajectories (blue in colour) converge to the critical point (0,0) (the big dot) as, $t \to \infty$ showing that the point is an attractor and locally asymptotically stable as explained in appendix B. The red curves are the boundaries of the physical and non-physical regions. This is mentioned above. The value of, H and, M we use for this plot is 1.5. The initial value for, x and, y we use is -3. From the trajectories around, P_0 we can see that it is stable as predicted analytically.

This is also clearly illustrated in figure 3.3.

For the second set of eigenvalues where, $H^2 = 4M^2$ we expect similar features as for the first set of eigenvalues. The only difference is that there is a separatrix for this case for the second set of eigenvalues. The features are shown in figure 3.4. This is explained in theorem B.2.3 of appendix B.

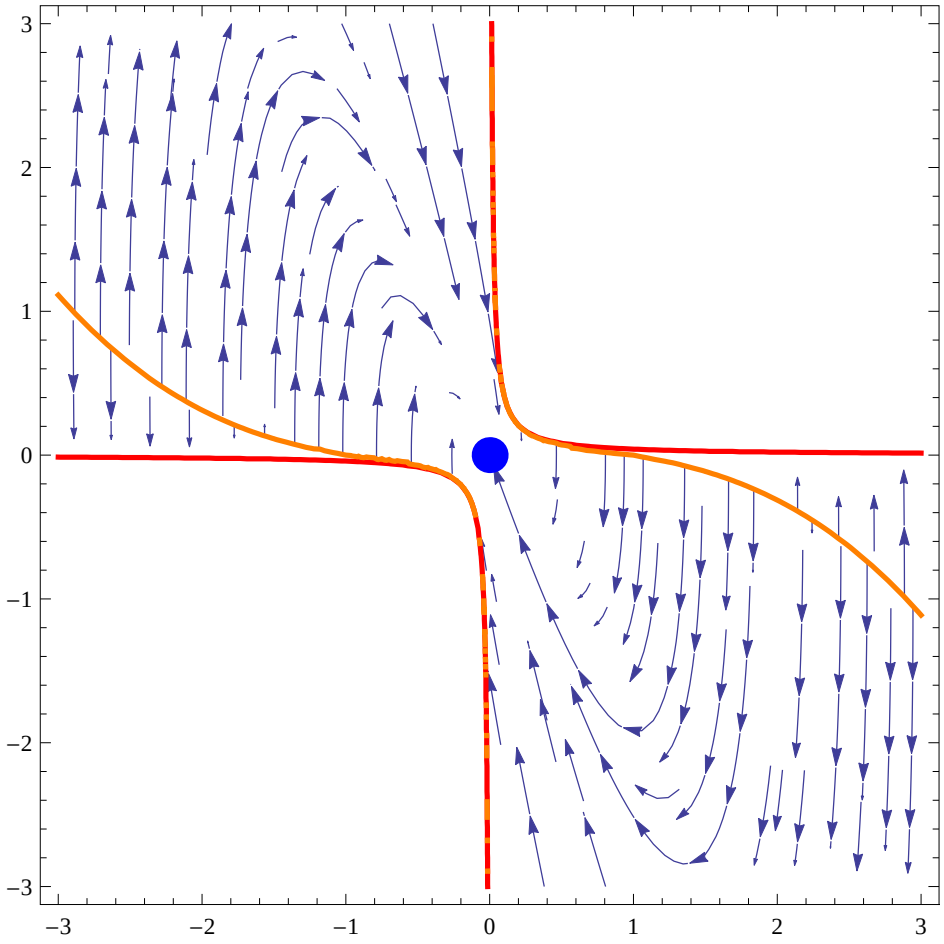

Figure 3.4: The second set of eigenvalues is considered for the case, $H^2 = 4M^2$. The orange curves is the separatrix which marks the boundary between the trajectories (blue in colour) that converge to the critical point (0,0) (the big dot) and those that do not as, $t \to \infty$. This is mentioned in the text. The red curves are the boundaries between the physical and non-physical regions. This is mentioned above. The values of, H and, M we use for this plot are 2 and 1 respectively. The initial value for, x and, y we use is -3. From the trajectories around, P_0 we can see that it is stable as predicted analytically. By studying the trajectories in the phase space corresponding to the orange separatrix and the boundary of the physical region, one can see that the orange separatrix asymptotically approaches the boundary of the non-physical and physical regions. The trajectories are approaching the boundary asymptotically.

For the same set where, $H^2 > 4M^2$ we expect similar features as for the first set (this is shown in theorem $B.2.1$ of appendix B). The only difference is that for the second set for this case there is a separatrix which marks the boundary between the trajectories that converge to the critical point (0,0) and those that do not as, $t \to \infty$. This is shown in figure 3.5.

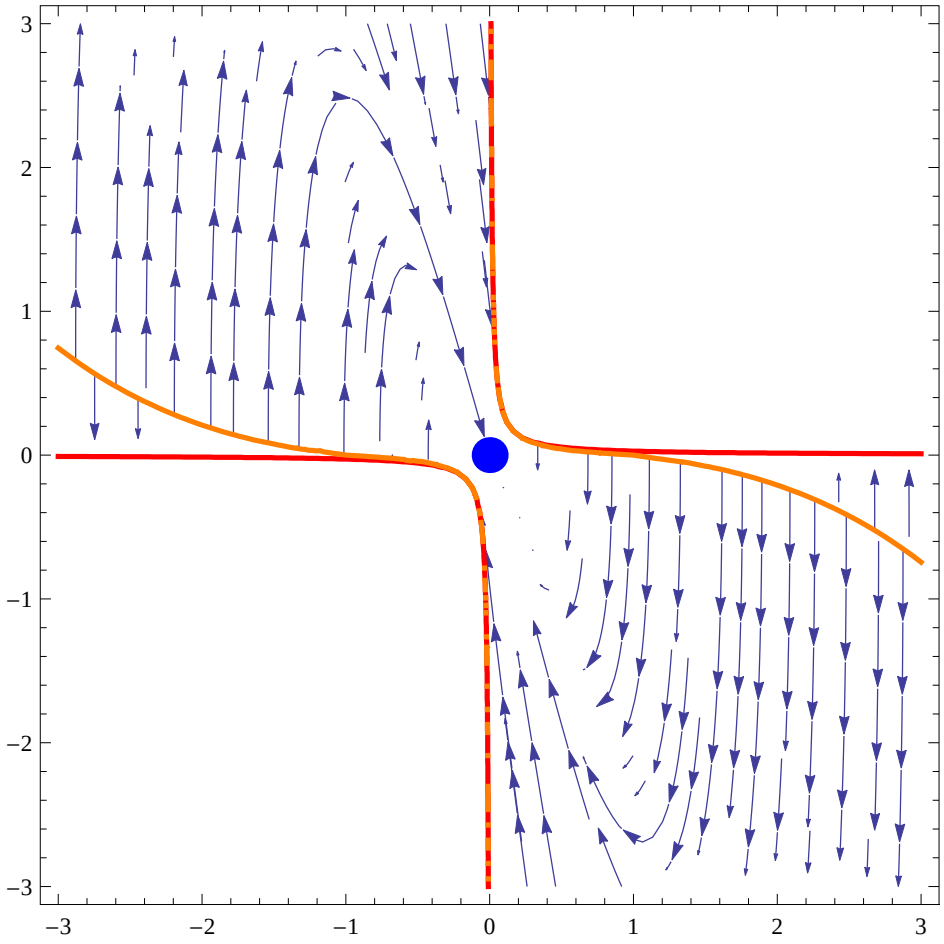

Figure 3.5: The second set of eigenvalues is considered for the case, $H^2 > 4M^2$. The orange curves is the separatrix which marks the boundary between the trajectories (blue in colour) that converge to the critical point (0,0) (the big dot) and those that do not as, $t \to \infty$. This is mentioned in the text. The red curves are the boundaries between the physical and non-physical regions. This is mentioned above. The values of, H and, M we use for this plot are 3 and 1 respectively. The initial value for, x and, y we use is -3. From the trajectories around, P_0 we can see that it is stable as predicted analytically. By studying the trajectories in the phase space corresponding to the orange separatrix and the boundary of the physical region, one can see that the orange separatrix asymptotically approaches the boundary of the non-physical and physical regions. The trajectories are approaching the boundary asymptotically.

But when, $H^2 < 4M^2$ we expect quite different features as shown in theorem $B.2.2$ of appendix B. For this case, the critical point is locally asymptotically stable since the real parts of the eigenvalues are negative (as explained in theorem $B.2.2$ of appendix B). The eigenvalues are complex (as shown in theorem $B.2.2$ of appendix B). Since the real parts are not equal to zero, we expect the system to be hyperbolic. Because of the imaginary part on the second set of eigenvalues, we expect to see periodic orbits of trajectories. The trajectories will circle around the fixed point (0,0) with period, $T = \frac{2\pi}{\omega}$. The trajectories are

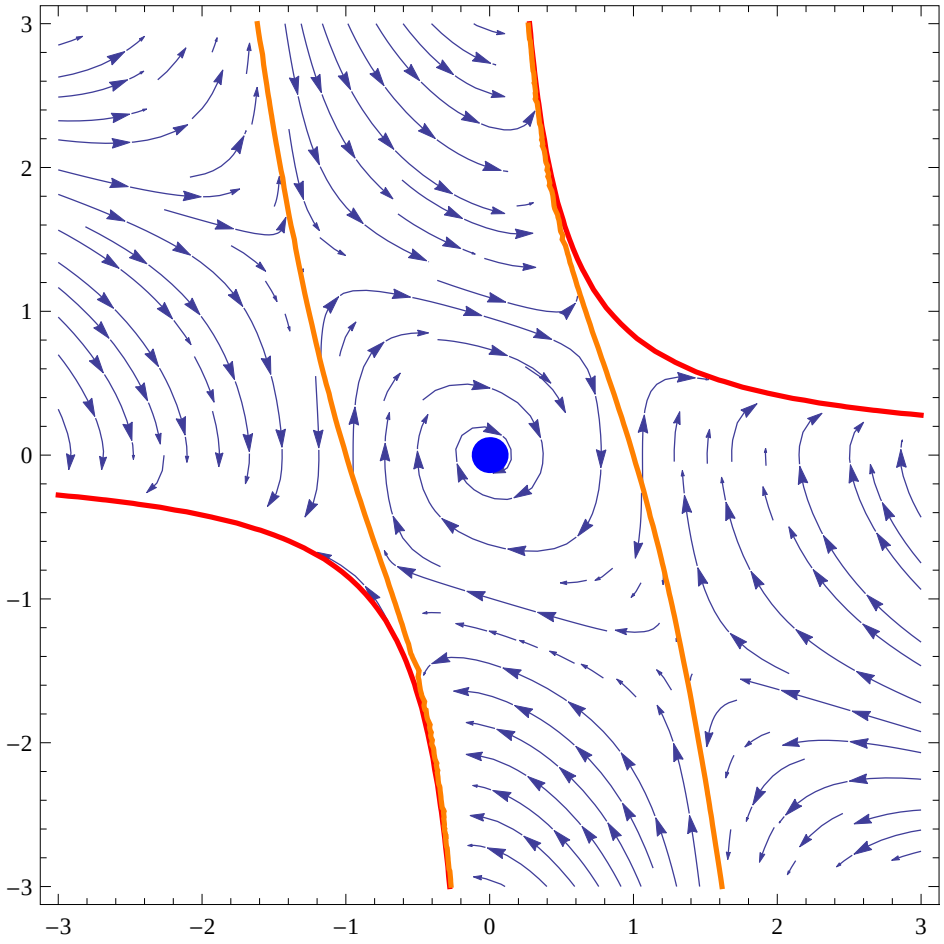

Figure 3.6: The second set of eigenvalues is considered for the case, $H^2 < 4M^2$. We see trajectories (blue in colour) spiralling toward, and converging to the critical point (0,0) (the big dot) as, $t \to \infty$. Hence, the critical point is an attractor and locally asymptotically stable as explained in the text. The red curves are the boundaries between the physical and non-physical regions. The orange straight lines are the $additional$ separatrices. The values of, H and, M we use for this plot are 10^{-1} and 1 respectively. The initial value for, x and, y we use is -3.

initially elliptical. With each revolution, their distances from the critical point (0,0) decay exponentially by a factor, $\exp[\lambda t]$ where, λ are the eigenvalues. The real parts are negative hence, the critical point (0,0) is a spiral sink (as explained in theorem $B.2.2$ of appendix B). Therefore, we expect the phaseportrait to show trajectories that spiral toward, and converge to the critical point (0,0) as, $t \to \infty$. This is clearly illustrated in figure 3.6.

- Separatrix $\frac{\epsilon B_z^2}{M^2} + \sqrt{1 - X} = 0$ for the case, $H^2 \geq 4M^2$. The separatrix marks the boundary between phasecurves or trajectories that converge to the critical point (0,0) and those that do not as, $t \to \infty$. This is shown in figures 3.4 and 3.5. By studying the trajectories in the phase space corresponding to the orange separatrix and the boundary of the physical

region in these figures 3.4 and 3.5, one can see that the orange separatrix asymptotically approaches the boundary of the non-physical and physical regions. The trajectories are approaching the boundary asymptotically.

- $1 - X = 0$. This is the curve for the boundary of the physical and non-physical regions. On the figures the curve is red.
- $1 - X < 0$. This is the non-physical region. It is there because of the square root sign in system 3.34. The trajectories or system are excluded there. The red curves in figures 3.3, 3.4, 3.5 and 3.6 mark the boundary between the non-physical and physical regions.
- $Additional$ separatrices on the phasemap for the case, $H^2 < 4M^2$. We do not know why and how these separatrices appear. These are shown in figure 3.6.

For this epoch, we obtain a critical point P_0. We linearise the system 3.34 around the point, P_0. We then obtain the first and second set of eigenvalues as shown in appendix B. From both sets of eigenvalues, we predict the features to expect on the phasemaps. In particular, we predict that, P_0 will be stable. We then obtain the expected phasemaps. After studying the trajectories near the critical point P_0 on the phasemaps we see that it is stable as expected. This is summarised in table 3.1.

Table 3.1: Stability of the Critical Point P_0

Summary of the stability of the critical point P_0 for the first and second set of eigenvalues for all values of, H and, M of given conditions.

P_0	[-2H,-H]	$H^2 = 4M^2$	$H^2 > 4M^2$	$H^2 < 4M^2$
Property	Stable	Stable	Stable	Stable

Table 3.1: In this table we summarise the features of the plots for the first set of eigenvalues in the first row and second column of the table and the second set of eigenvalues for the cases, $H^2 = 4M^2$, $H^2 > 4M^2$ and, $H^2 < 4M^2$. P_0 is the critical point. Property denotes the stability of, P_0 for the first set of eigenvalues and the stability of, P_0 for the second set of eigenvalues for all cases or scenarios. We find that the critical point P_0 is stable for all sets of eigenvalues in all scenarios.

The stability of the critical point P_0 thus illustrated. It is shown that the point is stable for the first and second set of eigenvalues irrespective of the values of, M and, H for the given conditions.

Endnote

It is shown that the critical point P_0 is stable for the first and second set of eigenvalues irrespective of the values of, M and, H for the given conditions.

Summary

We see that for the cases, $M^2 \gg H^2$ and, $M^2 \ll H^2$ the field oscillates with decaying amplitude for this epoch. We also see that the critical point P_0 is stable for the first and second set of eigenvalues irrespective of the values of, M and, H for the given conditions.

3.3 Radiation Dominated Epoch

3.3.1 Radiation Dominated Epoch for the Case, $M^2 \gg H^2$

During the radiation dominated epoch we have, $p = \frac{1}{2}$.

In the case, $M^2 \gg H^2$ and using, $\epsilon = -1$ we see that equation 3.22 reduces to:

$$\ddot{B}_z + 3H\dot{B}_z + M^2 B_z = 0. \tag{3.37}$$

The solution to equation 3.37 is equation 3.30. M^2 is the effective mass and, $3H > 0$ is the friction term. Since, $M^2 \gg 3H$ we can approximate equation 3.37 to:

$$\ddot{B}_z + M^2 B_z = 0, \tag{3.38}$$

whose solution is given by:

$$B_z \sim \exp\left[\int \sqrt{-M^2}dt\right]. \tag{3.39}$$

$M^2 > 0$, and so, $\sqrt{-M^2}$ is imaginary hence, the solution will oscillate. From, $3H > 0$ in equation 3.37 one expects the amplitude of oscillations to decay with time t. The general solution is given

by:

$$B_z \sim \frac{1}{\sqrt{3H}} \exp\left[\int \sqrt{-M^2}dt\right]. \tag{3.40}$$

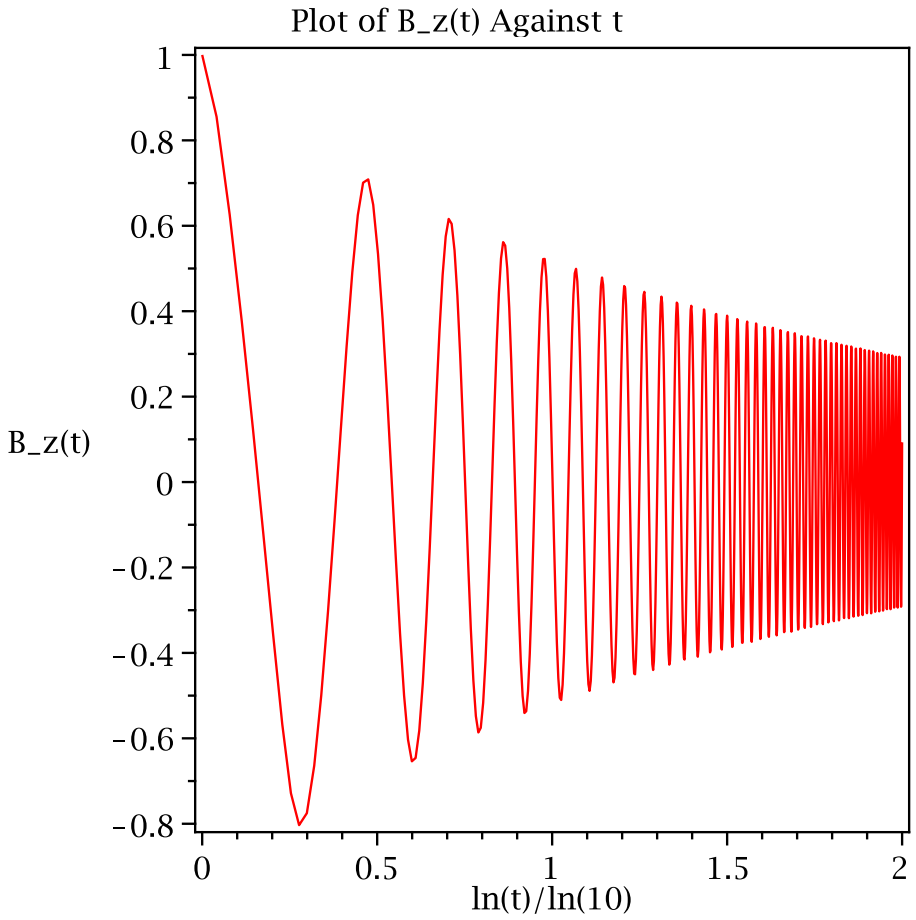

Figure 3.7: The case considered for this plot is, $M^2 \gg H^2$. We choose values that satisfy the case, $M^2 \gg H^2$. The value we use for, M is 1.2 and, $H = \frac{1}{2t}$ where $1 \leq t \leq 100$. The initial values for, B..z(t)= B_z and, $\dot{B}_z$ we use are 1 and 0 respectively. The field oscillations are decaying by a factor, $a^{-\frac{1}{2}}$.

This is explained in appendix A.

The full equation corresponding to, $p = \frac{1}{2}$ is:

$$\begin{aligned} 0 &= \left[\frac{\epsilon B_z^2}{M^2} + \sqrt{1-X}\right]\ddot{B}_z + 3H\left[\frac{\epsilon M^2}{36H^2}X + \sqrt{1-X}\right]\dot{B}_z \\ &- M^2\left[\frac{5\epsilon}{6} - \frac{2\epsilon}{3}X - \frac{1}{6}\sqrt{1-X}\right]B_z. \end{aligned} \tag{3.41}$$

We choose values that satisfy the case, $M^2 \gg H^2$. We then solve it numerically for, $M = 1.2$ and, $H = \frac{1}{2t}$ where $100 \geq t \geq 1$. The field oscillates as expected. As expected the amplitude decays by a factor of, $a^{-\frac{1}{2}}$. This is shown in figure 3.7.

For the same case, $M^2 \gg H^2$ and using, $\epsilon = +1$, equation 3.22 reduces to:

$$\ddot{B}_z + 3H\dot{B}_z - \frac{2}{3}M^2 B_z = 0. \tag{3.42}$$

Here, $\frac{2}{3}\left|-M^2\right| = \frac{2}{3}M^2$ is the effective mass and, $3H > 0$ is the friction term. Since, $\frac{2}{3}M^2 \gg 3H$, we can approximate equation 3.42 to:

$$\ddot{B}_z - \frac{2}{3}M^2 B_z = 0, \tag{3.43}$$

whose solution is given by:

$$B_z \sim \exp\left[\int \sqrt{\frac{2}{3}M^2}dt\right]. \tag{3.44}$$

Since, $-\frac{2}{3}M^2 < 0$, and so, $\sqrt{\frac{2}{3}M^2} \in \mathbb{R}$, the field will have an exponential behaviour. The general solution is given by:

$$B_z \sim \frac{1}{\sqrt{3H}}\exp\left[\int \sqrt{\frac{2}{3}M^2}dt\right]. \tag{3.45}$$

This is explained in appendix A.

We then solve the full equation 3.41 numerically. We choose values that satisfy the case, $M^2 \gg H^2$. For, $M = 35$ and, $H = \frac{1}{2t}$ where $100 \geq t \geq 1$, the field grows exponentially. This is shown in figure 3.8.

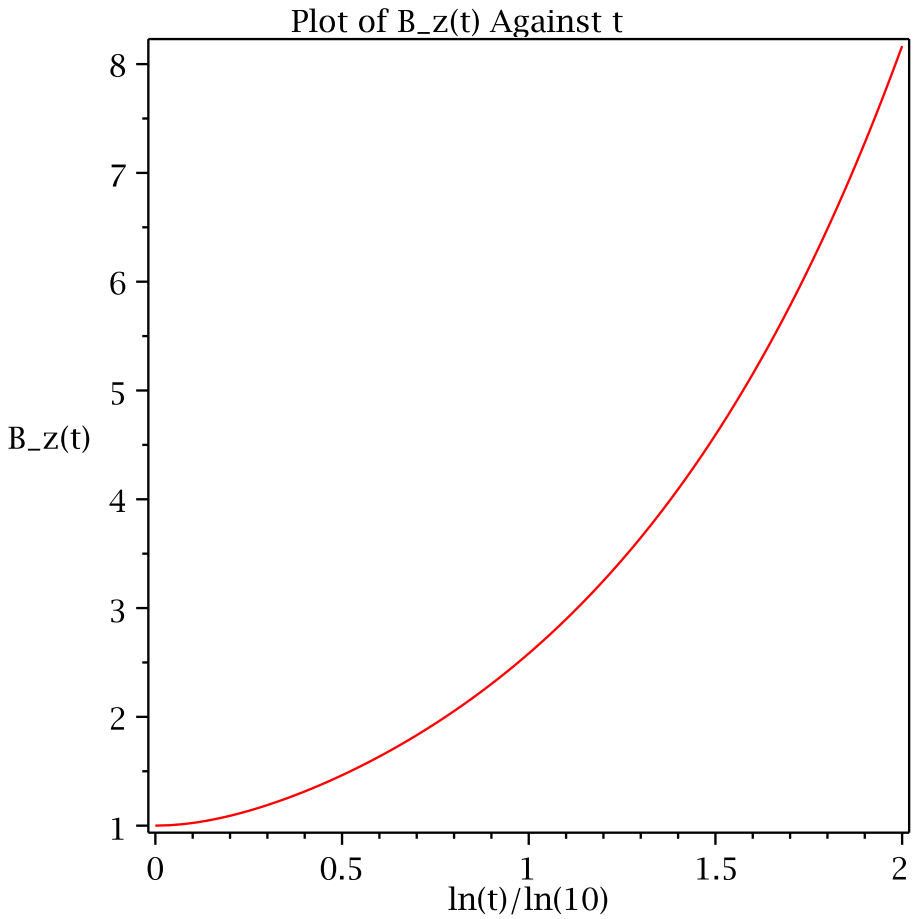

Figure 3.8: The case considered for this plot is, $M^2 \gg H^2$. The value we use for, M is 35 and, $H = \frac{1}{2t}$ where $1 \leq t \leq 100$. The initial values for, B..z(t)=B_z and, $\dot{B}_z$ we use are 1.0 and 0 respectively. The field then grows exponentially.

Endnote

It is shown that for the case, $M^2 \gg H^2$ the field either oscillates with decreasing amplitude or grows exponentially.

3.3.2 Other Analytical Methods for Radiation Dominated Epoch

For radiation and matter, it is not possible to reduce equations 3.41 and 3.56 respectively to an autonomous system. However, we can solve them analytically using other methods then compare with their numerical solutions.

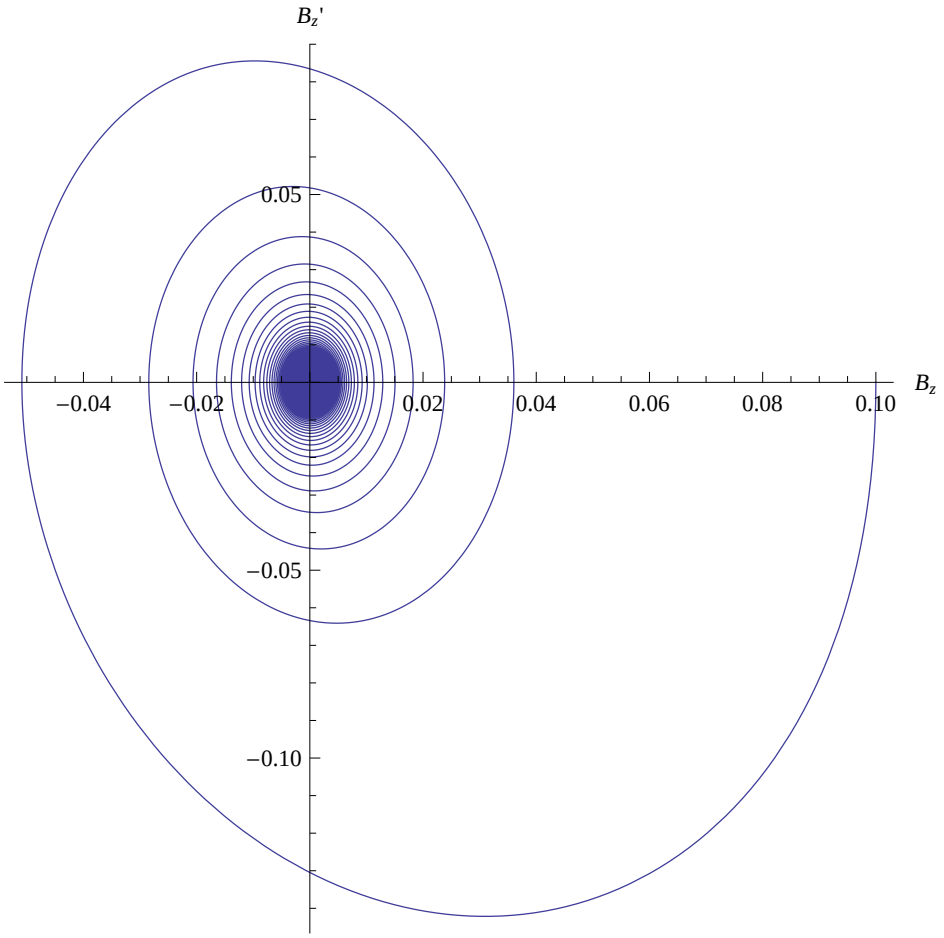

Figure 3.9: The case considered is, $M^2 \gg H^2$ implying that $4M^2 > 9H^2$. The value we use for, M is 2.0 and, $H = \frac{1}{2t}$ where $1 \leq t \leq 2,000$. The initial values for, B_z and, $\dot{B}_z = B_z'$ we use are 0.10 and 0 respectively. We then see trajectories near the point (0,0) moving or spiralling just around that point. This shows that the point (0,0) is stable as explained in the text.

We consider the case, $M^2 \gg H^2$. Using, $\epsilon = -1$, equation 3.22 reduces to:

$$\ddot{B}_z + 3H\dot{B}_z + M^2 B_z \;=\; 0. \tag{3.46}$$

The eigenvalues for equation 3.46 after solving its characteristic equation are:

$$\lambda_1 \;=\; \frac{-3H - \sqrt{9H^2 - 4M^2}}{2}, \tag{3.47}$$

and:

$$\lambda_2 \;=\; \frac{-3H + \sqrt{9H^2 - 4M^2}}{2}. \tag{3.48}$$

The solution to equation 3.46 is:

$$B_z = \exp\left[-\left(\frac{3H}{2}\right)t\right][c_1\cos\omega t + c_2\sin\omega t], \tag{3.49}$$

as equation 3.30 implying that:

$$\dot{B}_z = \exp\left[-\left(\frac{3H}{2}\right)t\right]\left[\left(c_2\omega - \frac{3H}{2}c_1\right)\cos\omega t - \left(c_1\omega + c_2\frac{3H}{2}\right)\sin\omega t\right], \tag{3.50}$$

where:

$$\omega = \frac{\sqrt{4M^2 - 9H^2}}{2}, \tag{3.51}$$

and, c_1, c_2 are constants. For eigenvalues 3.47 and 3.48 we can see that $4M^2 > 9H^2$ since, $M^2 \gg H^2$. Since this is the case, the eigenvalues are complex. Therefore, we expect oscillations. The oscillations are underdamped by the factor, $\exp\left[-\frac{3H}{2}t\right]$. Since, $3H > 0$ and $2 > 0$, we have, $-\left[\frac{3H}{2}\right] < 0$ so, $\exp\left[-\left(\frac{3H}{2}\right)t\right] \to 0$ as $t \to \infty$. This implies that, $B_z \to 0$ as, $t \to \infty$; that is, the field decays to 0 as time increases. This also implies that, $\dot{B}_z \to 0$ as, $t \to \infty$. Therefore, the point (0,0) should be the converging point on the phaseportrait. The real parts of the eigenvalues are negative. This implies that the trajectories should move (spiral) towards or just around the point (0,0) with a period of $T = \frac{2\pi}{\omega}$. The point (0,0) is then said to be a stable attractor. This is explained in appendix C.

We then solve equations 3.41 and 3.56 numerically. We choose values that satisfy the case, $M^2 \gg H^2$. For, $M = 2.0$ and, $H = \frac{1}{2t}$ for radiation where $2,000 \geq t \geq 1$, we see trajectories moving (spiralling) just around the point (0,0). There is damping as expected. The trajectories are elliptical originally. With each revolution, their distances from the point (0,0) decay exponentially according to $\exp[-0.75]$ for radiation. This is clearly illustrated in figure 3.9.

Endnote

It is shown that the point (0,0) on the phaseportrait 3.9 is stable.

Summary

For the case, $M^2 \gg H^2$ during this epoch, we see some of the interesting phenomenologies for the evolution of vector field self-interactions that are relatively related to $Galileon$ fields. We see that the field either grows exponentially or oscillates with decaying amplitude. We also see that the point (0,0) on the phaseportrait 3.9 is stable.

3.4 Matter Dominated Epoch

3.4.1 Matter Dominated Epoch for the Cases, $M^2 \gg H^2$ and, $M^2 \ll H^2$

In a universe that is dominated by a pressureless fluid, the scale factor a evolves as, $a \propto t^{\frac{2}{3}}$. $p = \frac{2}{3}$ for this case.

We first consider the case, $M^2 \ll H^2$. Equation 3.16 reduces to:

$$\ddot{B}_z + 3H\dot{B}_z + \frac{1}{2}H^2 B_z = 0, \tag{3.52}$$

where the effective mass is $m_{eff}^2 = \frac{1}{2}H^2$. The solution to equation 3.52 is:

$$B_z = c_1 \exp\left[-\frac{3H + H\sqrt{7}}{2}\right] + c_2 \exp\left[\frac{-3H + H\sqrt{7}}{2}\right], \tag{3.53}$$

where, c_1 and, c_2 are constants. Since, $m_{eff}^2 > 0$, we expect the field to oscillate and from the friction term $3H > 0$ we expect the amplitude of oscillations to decay asymptotically. This is explained in appendix A. For equation 3.52, $3H \gg \frac{1}{2}H^2$. This implies that it can be approximated to:

$$\ddot{B}_z + 3H\dot{B}_z = 0, \tag{3.54}$$

whose solution is given by:

$$\dot{B}_z \sim \exp\left[-\int 3H dt\right], \tag{3.55}$$

which is the amplitude of oscillatons. $3H > 0$ affects the amplitude of oscillations or, $\dot{B}_z$.

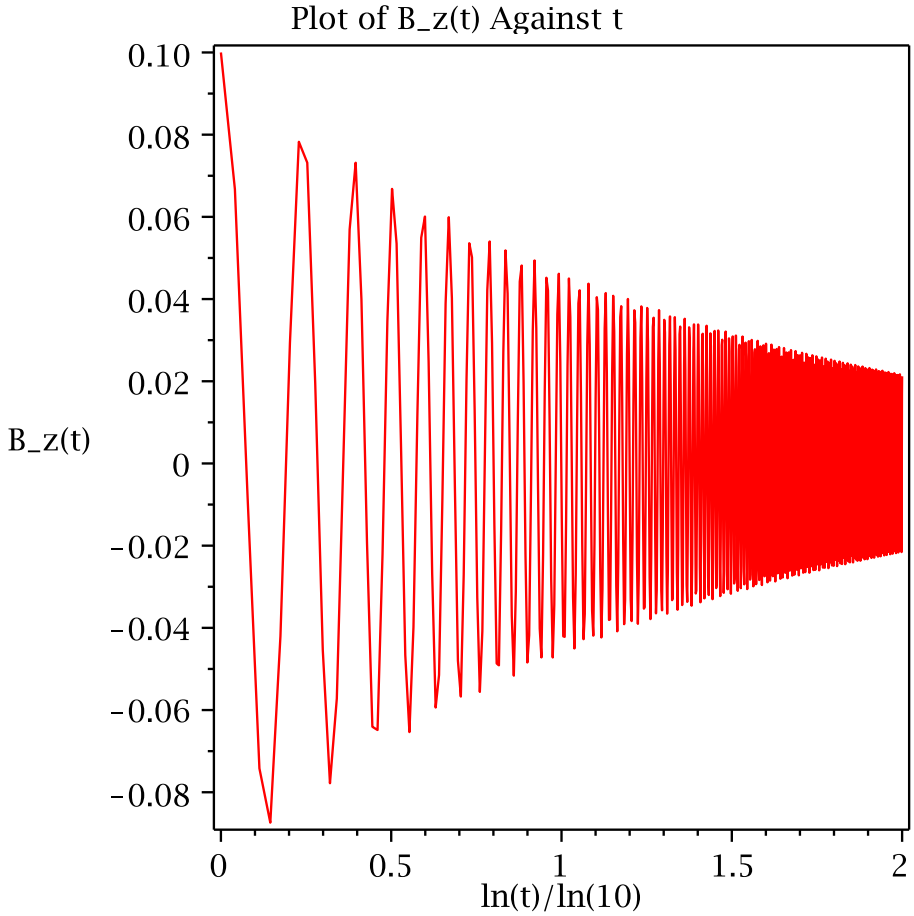

Figure 3.10: The case considered for this plot is, $M^2 \ll H^2$. The value we use for, M is 10^{-4} and, $H = \frac{2}{3t}$ where $1 \leq t \leq 100$. The initial values for, B..z(t)=B_z and, $\dot{B}_z$ we use are $\exp[-1]$ and 0 respectively. We then see field oscillations decaying by a factor, $a^{-\frac{1}{2}}$.

The full equation 3.9 that corresponds to, $p = \frac{2}{3}$ is:

$$\begin{aligned} 0 &= \left[\frac{\epsilon B_z^2}{M^2} + \sqrt{1-X}\right]\ddot{B}_z + 3H\left[\frac{\epsilon M^2}{36H^2}X + \sqrt{1-X}\right]\dot{B}_z \\ &- M^2\left[\frac{3\epsilon}{4} - \frac{5\epsilon}{8}X - \left(\frac{1}{4} + \frac{H^2}{2M^2}\right)\sqrt{1-X}\right]B_z. \end{aligned} \tag{3.56}$$

We choose values that satisfy the case, $M^2 \ll H^2$. We then solve it numerically for, $M = 10^{-4}$ and, $H = \frac{2}{3t}$ where $100 \geq t \geq 1$, and the field oscillates as expected. As expected the amplitude decays by a factor of, $a^{-\frac{1}{2}}$. This is shown in figure 3.10.

We now consider the case, $M^2 \gg H^2$.

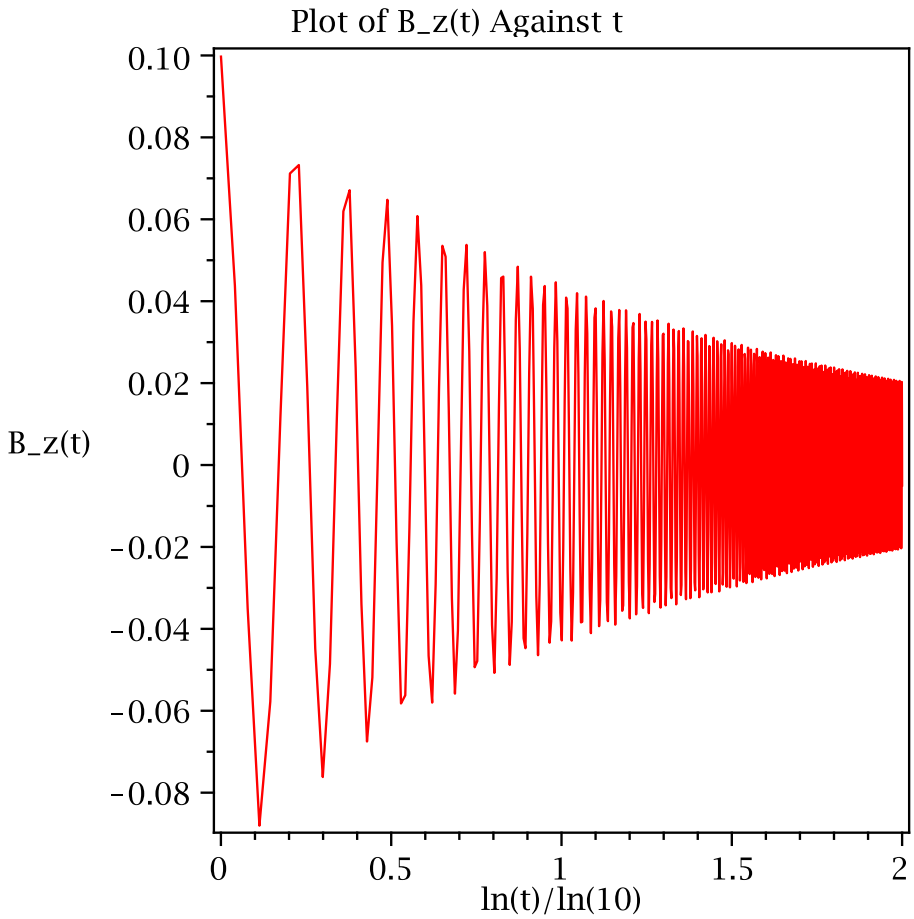

Figure 3.11: The case considered for this plot is, $M^2 \gg H^2$. The value we use for, M is 6.1 and, $H = \frac{2}{3t}$ where $1 \leq t \leq 100$. The initial values for, B..z(t)=B_z and, $\dot{B}_z$ we use are $\exp[-1]$ and 0 respectively. We then see field oscillations decaying by a factor, $a^{-\frac{1}{2}}$.

Using, $\epsilon = -1$, equation 3.22 reduces to:

$$\ddot{B}_z + 3H\dot{B}_z + M^2 B_z \;=\; 0. \tag{3.57}$$

The solution to equation 3.57 is equation 3.30. M^2 is the effective mass and, $3H > 0$ is the friction term. Since, $M^2 \gg 3H$, we can approximate equation 3.57 to:

$$\ddot{B}_z + M^2 B_z \;=\; 0, \tag{3.58}$$

whose solution is:

$$B_z \sim \exp\left[\int \sqrt{-M^2}dt\right]. \tag{3.59}$$

Now, $M^2 > 0$, and so, $\sqrt{-M^2}$ is imaginary hence, the solution will oscillate. Because of the friction term, $3H > 0$ in equation 3.57 we expect the amplitude of oscillations to decay asymptotically. The general solution is given by:

$$B_z \sim \frac{1}{\sqrt{3H}} \exp\left[\int \sqrt{-M^2} dt\right]. \tag{3.60}$$

A detailed explanation of this is given in appendix A.

We then solve the full equation 3.56 numerically. We choose numerical values that satisfy the case, $M^2 \gg H^2$. For, $M = 6.1$ and, $H = \frac{2}{3t}$ where $100 \geq t \geq 1$, the field oscillates as expected. As expected the amplitude decays by a factor of, $a^{-\frac{1}{2}}$. This is shown in figure 3.11.

Endnote

It is shown that the field oscillates with decreasing amplitude for the cases, $M^2 \gg H^2$ and, $M^2 \ll H^2$.

3.4.2 Other Analytical Methods for Matter Dominated Epoch

As explained above in subsection 3.3.2 for the radiation dominated epoch, the same is also done for the matter dominated epoch analytically.

We choose values that satisfy the case, $M^2 \gg H^2$. For this case we have, $M = 3.0$ and, $H = \frac{2}{3t}$ for matter where $9,000 \geq t \geq 1$, and we see trajectories moving (spiralling) just around the point $(0, 0)$. There is damping as expected. The trajectories are elliptical originally. With each revolution, their distances from the point $(0, 0)$ decay exponentially according to, $\exp[-1]$ for matter. This is also clearly illustrated in figure 3.12.

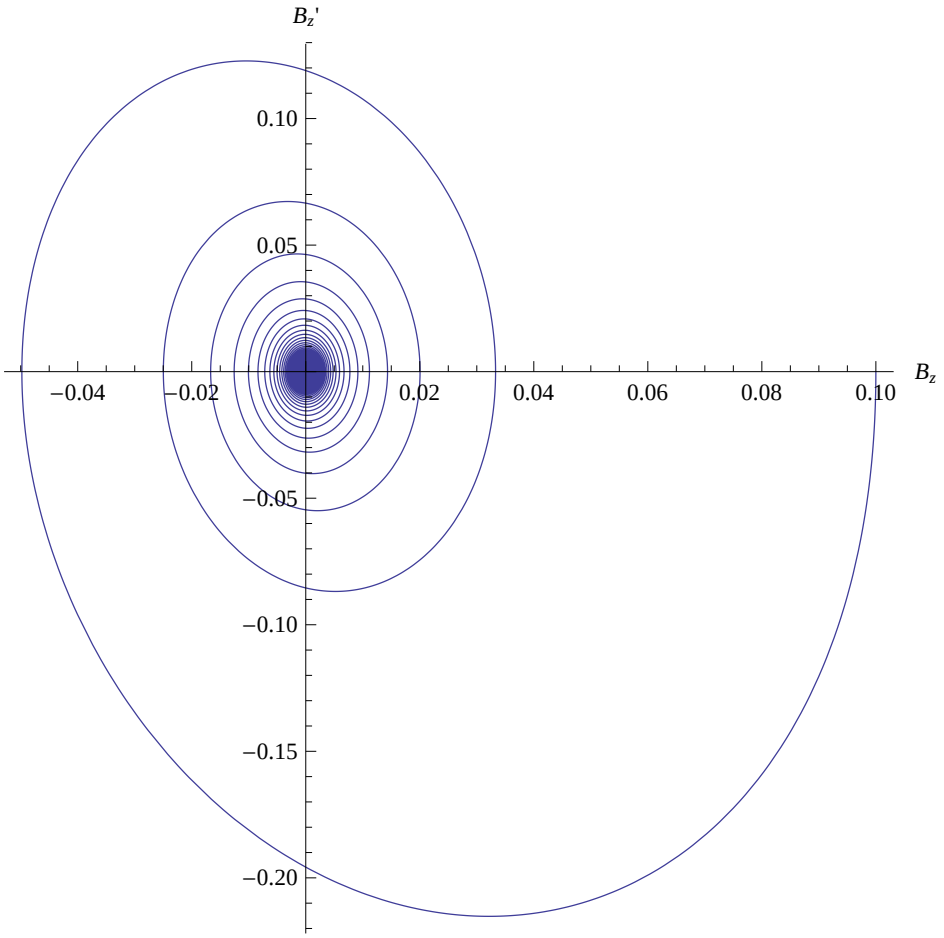

Figure 3.12: The case considered is, $M^2 \gg H^2$ implying that $4M^2 > 9H^2$. The value we use for, M is 3.0 and, $H = \frac{2}{3t}$ where $1 \leq t \leq 9,000$. The initial values for, B_z and, $\dot{B}_z = B_z'$ we use are 0.10 and 0 respectively. We then see trajectories near the point (0,0) moving or spiralling just around that point. This shows that the point (0,0) is stable as explained in the text.

Endnote

It is shown that the point (0,0) on the phaseportrait 3.12 is stable.

Summary

For the cases, $M^2 \gg H^2$ and, $M^2 \ll H^2$ during this epoch, we can see some of the interesting phenomenologies for the evolution of vector field self-interactions that are relatively related to $Galileon$ fields. We see that the field only oscillates with decaying amplitude. We also see that

the point (0,0) on the phaseportrait 3.12 is stable.

Table 3.2: Behaviour of the Field for the Cases, $M^2 \gg H^2$ and, $M^2 \ll H^2$ for all Epochs

A summary of the behaviour of vector field self-interactions that are relatively related to $Galileon$ fields is given in table 3.2 for the cases, $M^2 \gg H^2$ and, $M^2 \ll H^2$ for all epochs.

Property	Inflation	Radiation	Matter
Oscillating	$M^2 \ll H^2$	$M^2 \gg H^2$	$M^2 \ll H^2$
Oscillating	$M^2 \gg H^2$		$M^2 \gg H^2$
Growing		$M^2 \gg H^2$	

Table 3.2: In this table we summarise the features of the plots for the two cases, $M^2 \gg H^2$ and, $M^2 \ll H^2$. Oscillating means that the field oscillates with decaying amplitude. Growing means that the field grows exponentially. For these cases we see that the field either oscillates with decreasing amplitude or grows exponentially.

The behaviour of the field thus illustrated for the cases, $M^2 \gg H^2$ and, $M^2 \ll H^2$ for all epochs. The field either oscillates with decreasing or decaying amplitude or grows exponentially.

Final Remarks

For the cases, $M^2 \gg H^2$ and, $M^2 \ll H^2$ for all epochs, we see that the field either oscillates with decreasing amplitude or grows exponentially. We also see that the point (0,0) on all phasemaps for all epochs is stable.

General Final Remarks

We see that the field either oscillates with decreasing amplitude or grows exponentially for the cases, $M^2 \gg H^2$ and, $M^2 \ll H^2$. Table 3.2 summarises or illustrates the behaviour of the field for all epochs for the cases, $M^2 \gg H^2$ and, $M^2 \ll H^2$. Despite $additional$ separatrices

appearing on one of the plots for the inflationary epoch, we see that the point (0,0) is stable for all phasemaps for all epochs. For our future work, we will try to find out why and how these $additional$ separatrices appear on one of the plots for the inflationary epoch. We also need to study the stability of the trajectories near the separatrix in figures 3.4 and 3.5 for the inflationary epoch.

Chapter 4. Discussions and Conclusions

A discussion of the state of standard cosmology is presented in the first chapter. The universe is largely homogeneous and isotropic [71]. It began by some unknown mechanism, from an extremely hot and dense state which was characterised by rapid expansion [73, 101]. It progressed into an epoch of inflation which was rapid [51]. The cooling of energy content of the universe is believed to be due to this rapid inflation [51]. It was also proposed as a resolution to problems such as the monopole, flatness and horizon problems [51]. Rapid inflation happened because of a form of potential energy called the inflaton field potential energy [51]. It eventually decayed into relativistic particles described by the standard model of particle physics ($SMPP$) [51]. This led to the end of the inflationary epoch, and the beginning of the radiation dominated epoch [51]. This process is called reheating [53].

From the beginning of the radiation dominated epoch, the universe has continued to expand according to the dominating energy form in it [51]. Most recently, it has been observed that what seems to be an unclustered fluid having negative pressure is forcing the universe into a phase of accelerated expansion [51]. It is called Dark Energy (DE) [51].

There are serious problems in cosmology and modern physics that need to be resolved such as the mystery of the nature of DE. It is possible that our assumptions or laws of physics are wrong [51].

There are two major reasons to be skeptical about standard cosmology [51]:

(i) we can assume that the cosmological principle is correct, but GR is not complete.

(ii) we can assume that GR is correct, and abandon the assumptions of isotropy and homogeneity.

Alternative gravity is a field of research that considers the former [51]. Its goal is to generalise the field equations of GR so that it can explain the late time accelerated expansion of the universe [51]. In this thesis, a specific branch of alternative gravity is considered. It is called $Vector - Galileon - Tensor$ Theories of Gravity.

In the third chapter we develop a study of the cosmological evolution of a vector field non-minimally coupled to gravity and with a potential and a $Galileon$-motivated interaction terms.

We give the evolution of this field in terms of the parameters of the theory for the different epochs of the expansion history of the universe, namely: inflationary epoch, radiation dominated epoch and matter dominated epoch. We show that it is possible to obtain a wide variety of behaviours or interesting phenomenologies for the cosmological evolution of the field by choosing suitable values for the parameters, M and, H of given conditions. In particular, we obtain conditions for the parameters so that the field grows exponentially or oscillates (for oscillations the amplitude decays for all epochs) with time t. We obtain an autonomous system for the inflationary epoch. The general features of the phasemaps are given and the critical point is appropriately characterised. For radiation and matter epochs, it is not possible to reduce equations 3.41 and 3.56 respectively to an autonomous system. However, we solve them analytically using other methods then we compare with the numerical solutions of equations 3.41 and 3.56. The results match. In addition to the general results commented above, for the inflationary epoch, we also find a separatrix, curve for the boundary between the physical and non-physical regions, non-physical region and $additional$ separatrices. The separatrix marks the boundary between phasecurves or trajectories that converge to the critical point (0,0) and those that do not. For the non-physical region, the trajectories or system are excluded there. We would like to remark that throughout this work, we focus on vector field self-interactions that can give interesting phenomenologies for the cosmological evolution and that are relatively related to $Galileon$ fields for the different eras in the expansion history of the universe, namely: inflationary epoch, radiation dominated epoch and matter dominated epoch. For our future work, we need to find out how and why $additional$ separatrices appear in figure 3.6 for the inflationary epoch. We also need to study the stability of the trajectories near the separatrix in figures 3.4 and 3.5 for the inflationary epoch. One last comment, although throughout this work we focus on vector field self-interactions that are relatively related to $Galileon$ fields for the different eras in the expansion history of the universe, namely: inflationary epoch, radiation dominated epoch and matter dominated epoch, we would like to mention that due to their generality, the results given in this thesis can also be used in other cosmological contexts in which vector field self-interactions that are relatively related to $Galileon$ fields could play a very useful role.

Appendix A. Some General Features of Second-Order Differential Equations

---

We are given that:

$$\ddot{B}_z + \alpha \dot{B}_z + \beta B_z \;\; = \;\; 0, \tag{1.1}$$

where, α is the friction term (which affects the amplitude of oscillations by decreasing it) and, β is the effective mass. If, $\beta > 0$ we expect the field to oscillate while if, $\beta < 0$, we expect the field to have an exponential behaviour. If, $\beta \gg \alpha$, we can approximate appendix A equation 1.1 to:

$$\ddot{B}_z + \beta B_z \;\; = \;\; 0, \tag{1.2}$$

whose solution is given by:

$$B_z \sim \exp\left[\int \sqrt{-\beta} dt\right]. \tag{1.3}$$

Thus, if, $\beta > 0$, we have, $\sqrt{-\beta}$ as imaginary and the solution will oscillate. The term, α will affect the amplitude of the oscillations. The general solution is given by:

$$B_z \sim \frac{1}{\sqrt{\alpha}} \exp\left[\int \sqrt{-\beta} dt\right]. \tag{1.4}$$

If, $\beta < 0$, $\sqrt{-\beta} \in \mathbb{R}$, then the field will have an exponential behaviour. But if, $\beta \ll \alpha$ where, $\beta > 0$, we can approximate appendix A equation 1.1 to:

$$\ddot{B}_z + \alpha \dot{B}_z \;\; = \;\; 0, \tag{1.5}$$

whose solution is given by:

$$\dot{B}_z \sim \left[-\int \alpha dt\right], \tag{1.6}$$

which is the amplitude of oscillations. α affects the amplitude of oscillations, $\dot{B}_z$ by decreasing it.

Appendix B. Dynamical Systems

B.1 Dynamical Systems: Definition

Let, $x = [x_1, ...x_n]$ be a point in, n-dimensional space, $\overline{R^n}$ that traces out a curve through time [78, 79, 104, 106]. We can then describe this as, $x = x[t]$ where, $x[t] = [x_1(t), ..., x_n(t)]$ for $-\infty < t < \infty$ [78, 79, 104, 106].

Usually we do not know, $x[t]$ directly, but we do know the forces determining its rate and direction of change in some region of, $\overline{R^n}$ [78, 79, 104, 106]. We therefore, have [78, 79, 104, 106]:

$$\dot{\overline{x}} \quad = \quad f[\overline{x}], \overline{x} \in \overline{R^n} \tag{2.1}$$

where the dot indicates the derivative with respect to time t, so, $\dot{\overline{x}} = \frac{d\overline{x}}{dt}$. We can make the assumption that, f has continous partial derivatives [78, 79, 104, 106]. Writing those vector equations out in full, we get, $\frac{d\overline{x_1}}{dt} = f^1[\overline{x_1}, ..., \overline{x_n}], \frac{d\overline{x_2}}{dt} = f^2[\overline{x_1}, ..., \overline{x_n}], ..., \frac{d\overline{x_n}}{dt} = f^n[\overline{x_1}, ..., \overline{x_n}]$ [78, 79, 104, 106]. This can be called a set of $first - order$ ordinary differential equations in, n unknowns [78, 79, 104, 106]. It is $first - order$ because as we can see, no derivative higher than the first appears [78, 79, 104, 106]. It is $ordinary$ as opposed to $partial$ because as we can see, we want to solve for a function of the single variable, t, as opposed to solving for a function with several different variables [78, 79, 104, 106].

We call, $\overline{x[t]}$ a dynamical system if it satisfies the set of ordinary differential equations described above, in the sense that, $\dot{\overline{x[t]}} = f[\overline{x(t)}]$ for, t in some (possibly infinite) interval [78, 79, 104, 106]. A fixed point or a critical point or a stationary point, is a point, $\overline{x^*} \in \overline{R^n}$ for which, $f[\overline{x^*}] = 0$ [78, 79, 104, 106].

B.2 Dynamical Systems in Two Dimensions

The equations for a dynamical system in two dimensions can be written as [78, 79, 104, 106]:

$$\begin{aligned} \dot{x} &= f[x,y], \\ \dot{y} &= g[x,y]. \end{aligned} \tag{2.2}$$

Assuming, (x^*, y^*) is a fixed point [78, 79, 104, 106]. We can then write the $Jacobian$ of the system at this point [78, 79, 104, 106] in the form

$$A = \begin{bmatrix} a_{11} & a_{12} \\ a_{21} & a_{22} \end{bmatrix},$$

or

$$A = \begin{bmatrix} f_x(x^*, y^*) & f_y(x^*, y^*) \\ g_x(x^*, y^*) & g_y(x^*, y^*) \end{bmatrix}.$$

The linearisation of the dynamical system about, (x^*, y^*) can then be written in the form [78, 79, 104, 106]:

$$\dot{\overline{x}} = A\overline{x}, \tag{2.3}$$

where, $\overline{x}$ is the column vector:

$$\begin{bmatrix} x \\ y \end{bmatrix}.$$

Let us assume that, α =trace of $\frac{A}{2} = \frac{[a_{11}+a_{22}]}{2}$, β=det$[A] = a_{11}a_{22} - a_{21}a_{12}$, and $\gamma = \alpha^2 - \beta$, the discriminant of, A [78, 79, 104, 106]. It is easy to see that the eigenvalues of appendix B equation $(B.2.3)$ are, $\lambda_1 = \alpha + \sqrt{\gamma}$ and, $\lambda_2 = \alpha - \sqrt{\gamma}$ [78, 79, 104, 106]. We should take note that if, $\beta = 0$, the two equations in appendix B equation $(B.2.3)$ are multiples of each other, so the system is indeterminate [78, 79, 104, 106]. We can then assume that, $\beta \neq 0$, which implies that appendix B equation $(B.2.3)$ has the unique critical point $(0, 0)$ [78, 79, 104, 106]. We then have the following theorems [78, 79, 104, 106].

B.2.1 Theorem. *If, $\gamma > 0$, the dynamical system appendix B equation $(B.2.3)$ is governed by the following set of equations:*

$$x[t] = a\exp[\lambda_1 t] + b\exp[\lambda_2 t], \tag{2.4}$$

$$y[t] \quad = \quad c\exp[\lambda_1 t] + d\exp[\lambda_2 t], \tag{2.5}$$

for constants, a, b, c, and, d that depend on the initial conditions. We then see that the dynamical system is hyperbolic with distinct eigenvalues, $\lambda_1 = \alpha + \sqrt{\gamma}$ and $\lambda_2 = \alpha - \sqrt{\gamma}$.

It follows that if, $\lambda_1, \lambda_2 < 0$, the fixed point at $(0,0)$ is said to be globally stable. It is called a node and it is stable.

The phase diagram for a stable node in the case, $\gamma > 0$ is simple: the trajectories all converge to the fixed point and they are continous and not self intersecting, though not generally closed.

B.2.2 Theorem. *If, $\gamma < 0$, the dynamical system appendix B equation $(B.2.3)$ is then satisfied by the equations:*

$$x[t] \quad = \quad \exp[\alpha t][a\cos\omega t + b\sin\omega t], \tag{2.6}$$

$$y[t] \quad = \quad \exp[\alpha t][c\cos\omega t + d\sin\omega t], \tag{2.7}$$

where, $\omega = \sqrt{\gamma}$. The system is said to be hyperbolic if and only if, $\alpha \neq 0$, and its eigenvalues are therefore, $\lambda = \alpha \pm \omega\sqrt{-1}$, so trajectories circle around the fixed point with period $T = \frac{2\pi}{\omega}$.

If, $\alpha < 0$, the fixed point is said to be globally stable. This is then called a stable focus.

B.2.3 Theorem. *If, $\gamma = 0$, the dynamical system appendix B equation $(B.2.3)$ satisfies the set of equations:*

$$x[t] \quad = \quad \exp[\alpha t][at + b], \tag{2.8}$$

$$y[t] \quad = \quad \exp[\alpha t][ct + d]. \tag{2.9}$$

The system has the single eigenvalue α, and it is then said to be hyperbolic if and only if, $\alpha \neq 0$.

If, $\alpha < 0$, the origin is said to be a stable node.

The features of the phase diagram for this case is similar to that where, $\gamma > 0$.

B.2.4 Theorem. *The Hartman-Grobman Theorem*

Let us assume that, x^*, y^* is a hyperbolic critical point (meaning the real part of the eigenvalues of the $Jacobian$ matrix are not zero). Then this would mean that the phase diagrams of the

linearised and the non-linear systems are locally homeomorphic. This implies that the phase diagrams of the linearised and non-linear equations are similar given that none of the eigenvalues of the linearised have zero real part or the behaviour of the trajectories or phasecurves near the critical point of the linearised and the non-linear systems is similar.

For example, as explained above in this appendix, for the linearised system of equation 3.28, we have:

$$\begin{aligned} \dot{x} &= y, \\ \dot{y} &= -[2H^2 + M^2]x - 3Hy, \end{aligned} \tag{2.10}$$

hence, figure B.1 after numerical analysis.

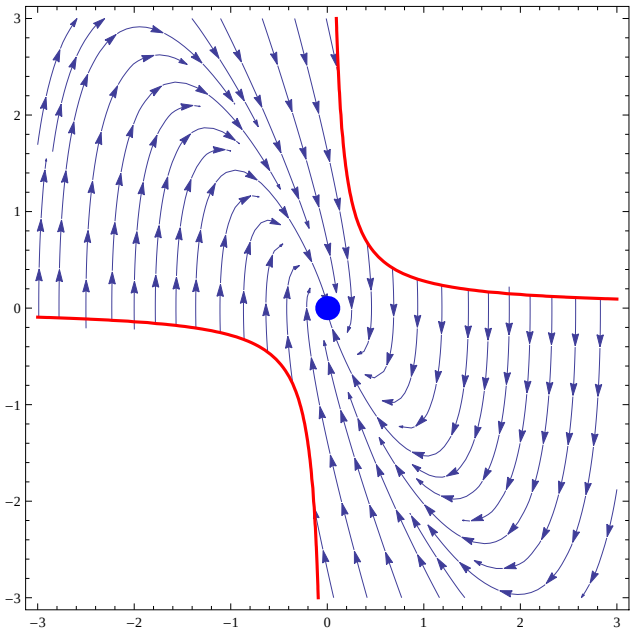

Figure B.1: Tajectories (blue in colour) near the critical point (0,0) (big dot) showing same or similar behaviour with the trajectories near the critical point of the non-linear system in figure 3.3. The features such as the red curves are the same or similar too. The value of, H and, M we use is 1.5. The initial value for, x and, y we use is -3.

For the same system 2.10 (B.2.10) after numerical analysis, we have figures B.2, B.3 and finally, figure B.4.

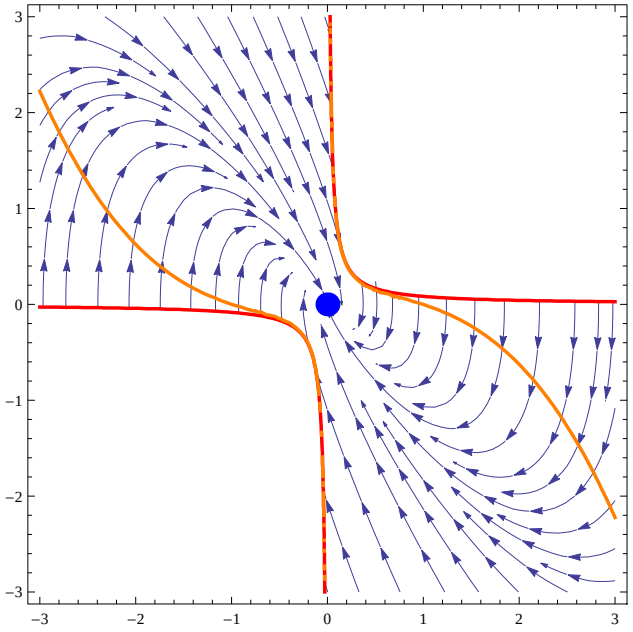

Figure B.2: Trajectories (blue in colour) near the critical point (0,0) (big dot) showing same or similar behaviour with trajectories near the critical point of the non-linear system in figure 3.4. The features such as the red curves are the same or similar too. The values of, H and, M we use are 2.0 and 1 respectively. The initial value for, x and, y we use is -3.

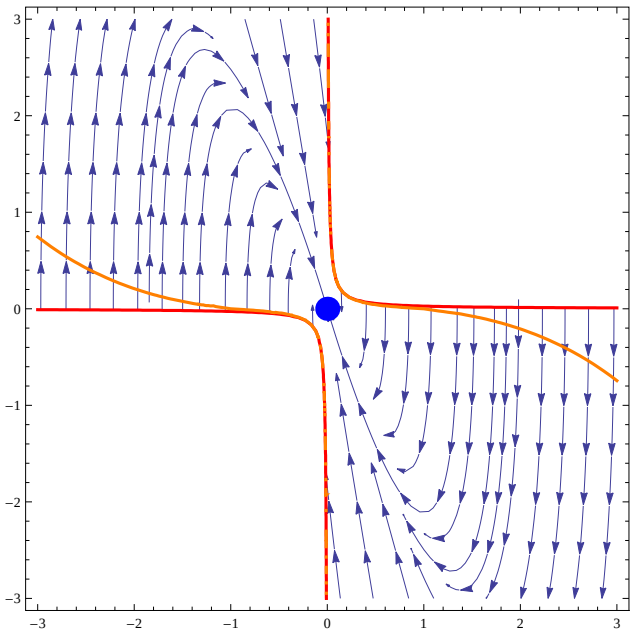

Figure B.3: Trajectories (blue in colour) near the critical point (0,0) (big dot) showing same or similar behaviour with trajectories near the critical point of the non-linear system in figure 3.5. The features such as the red curves are the same or similar too. The values of, H and, M we use are 3.0 and 1 respectively. The initial value for, x and, y we use is -3.

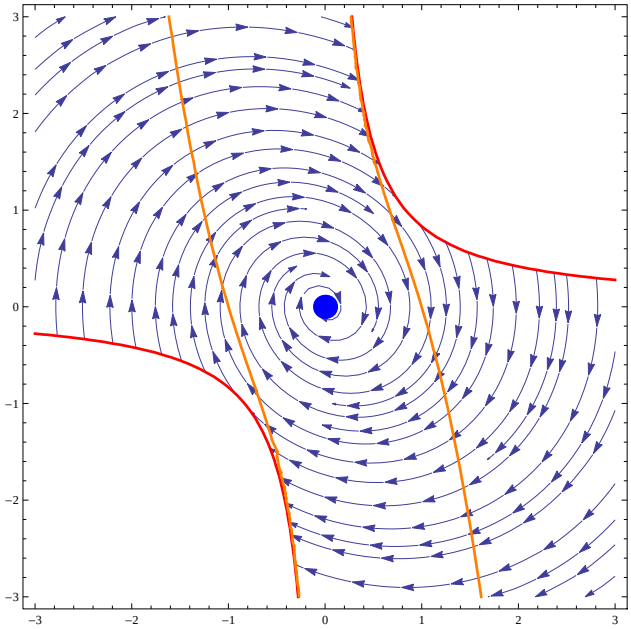

Figure B.4: Trajectories (blue in colour) near the critical point (0,0) (big dot) showing same or similar behaviour with trajectories near the critical point of the non-linear system in figure 3.6. The features such as the red curves are the same or similar too. The values of, H and, M we use are 10^{-1} and 1.0 respectively. The initial value for, x and, y we use is -3.

The two equations in 2.10 (B.2.10) can be combined leading to the following equation which is:

$$\frac{dy}{dx} = -[2H^2 + M^2]\frac{x}{y} - 3H, \tag{2.11}$$

for the trajectories on the phase maps above.

Appendix C. Applications of Second-Order Differential Equations

In science and engineering, second-order linear differential equations are applied in a variety of ways. We will consider one of them: the vibration of springs [41, 63].

Damped Vibrations

We consider the motion of a spring that is subject to a frictional force or a damping force.

It is assumed that the damping force is proportional to the velocity of the mass and acts in the direction that is opposite to the motion [41, 63]. Hence [41, 63]:

$$damping - force = -c\frac{dx}{dt}, \tag{3.1}$$

where, c is a positive constant, called the damping constant. Hence, in this case, $Newton's$ second law gives [41, 63]:

$$\begin{aligned} m\frac{d^2x}{dt^2} &= restoring - force + damping - force, \\ &= -kx - c\frac{dx}{dt}, \end{aligned} \tag{3.2}$$

or:

$$m\frac{d^2x}{dt^2} + c\frac{dx}{dt} + kx = 0. \tag{3.3}$$

We can see that appendix C equation 3.3 $(C.3.3)$ is a second-order linear differential equation and its auxilliary equation is $mr^2 + cr + k = 0$ [41, 63]. The roots are given by [41, 63]:

$$r_1 = \frac{-c + \sqrt{c^2 - 4mk}}{2m}, \tag{3.4}$$

and:

$$r_2 = \frac{-c - \sqrt{c^2 - 4mk}}{2m}. \tag{3.5}$$

We then discuss one case.

The case is where $c^2 - 4mk < 0$ (underdamping).

Here we can easily see that the roots are complex [41, 63]:

$$r_1 = -\frac{c}{2m} + \omega i, \tag{3.6}$$

or:

$$r_2 = -\frac{c}{2m} - \omega i, \tag{3.7}$$

where:

$$\omega = \frac{\sqrt{4mk - c^2}}{2m}. \tag{3.8}$$

Using $Euler's$ equation [41, 63]:

$$\exp[i\theta] = \cos\theta + i\sin\theta, \tag{3.9}$$

we can write the solution of the differential equation as:

$$\begin{aligned} x &= C_1 \exp[r_1 t] + C_2 \exp[r_2 t], \\ &= C_1 \exp\left[\left(-\frac{c}{2m} + i\omega\right)t\right] + C_2 \exp\left[\left(-\frac{c}{2m} - i\omega\right)t\right], \\ &= C_1 \exp\left[\left(-\frac{c}{2m}\right)t\right][\cos\omega t + i\sin\omega t] + C_2 \exp\left[\left(-\frac{c}{2m}\right)t\right][\cos\omega t - i\sin\omega t], \\ &= \exp\left[\left(-\frac{c}{2m}\right)t\right][(C_1 + C_2)\cos\omega t + i(C_1 - C_2)\sin\omega t]. \end{aligned} \tag{3.10}$$

This then results in [41, 63]:

$$x = \exp\left[\left(-\frac{c}{2m}\right)t\right][c_1\cos\omega t + c_2\sin\omega t], \tag{3.11}$$

where, $c_1 = C_1 + C_2$, $c_2 = i[C_1 - C_2]$. The oscillations are damped by the factor, $\exp\left[\left(-\frac{c}{2m}\right)t\right]$ [41, 63]. Since, $c > 0$ and, $m > 0$, we have that, $-\left[\frac{c}{2m}\right] < 0$ so, $\exp\left[-\left(\frac{c}{2m}\right)t\right] \to 0$ as, $t \to \infty$ [41, 63]. This means that, $x \to 0$ as, $t \to \infty$; that is, the motion decays to 0 as time t increases [41, 63].

References

[1] P. Ade, O. Doré, G. Helou, S. Hildebrandt, T. Pearson, G. Prézeau, G. Rocha, M. Seiffert, R.-R. Chary, P. McGehee, et al. Planck 2015 results. xiii. cosmological parameters. 2015.

[2] A. Albrecht and P. J. Steinhardt. Cosmology for grand unified theories with radiatively induced symmetry breaking. *Physical Review Letters*, 48(17):1220, 1982.

[3] L. Amendola and S. Tsujikawa. *Dark energy: theory and observations*. Cambridge University Press, 2010.

[4] C. Armendariz-Picon and A. Diez-Tejedor. Aether unleashed. *Journal of Cosmology and Astroparticle Physics*, 2009(12):018, 2009.

[5] T. Banks. Susy breaking, cosmology, vacuum selection and the cosmological constant in string theory. *arXiv preprint hep-th/9601151*, 1996.

[6] J. M. Bardeen, P. J. Steinhardt, and M. S. Turner. Spontaneous creation of almost scale-free density perturbations in an inflationary universe. *Physical Review D*, 28(4):679, 1983.

[7] N. Barnaby. *Cosmological Instabilities*. PhD thesis, McGill University, 2007.

[8] J. Bekenstein. Phys. rev. d70, 083509 (2004). *arXiv preprint astro-ph/0403694*.

[9] P. G. Bergmann. Comments on the scalar-tensor theory. *International Journal of Theoretical Physics*, 1(1):25–36, 1968.

[10] V. Bhatia, S. Misra, and N. Panchapakesan. Galactic gamma-ray background as a constraint on millisecond pulsars. *The Astrophysical Journal*, 476(1):238, 1997.

[11] E. Bianchi and C. Rovelli. Why all these prejudices against a constant? *arXiv preprint arXiv: 1002.3966*, 2010.

[12] R. Bluhm and V. A. Kostelecký. Spontaneous lorentz violation, nambu-goldstone modes, and gravity. *Physical Review D*, 71(6):065008, 2005.

[13] C. Brans and R. H. Dicke. Mach's principle and a relativistic theory of gravitation. *Physical Review*, 124(3):925, 1961.

[14] S. Capozziello and V. Faraoni. *Beyond Einstein gravity: A Survey of gravitational theories for cosmology and astrophysics*, volume 170. Springer Science & Business Media, 2010.

[15] B. Carr. *Universe or multiverse?* Cambridge University Press, 2007.

[16] S. M. Carroll. An introduction to general relativity. *Spacetime and Geometry*, 2004.

[17] S. M. Carroll, V. Duvvuri, M. Trodden, and M. S. Turner. Is cosmic speed-up due to new gravitational physics? *arXiv preprint astro-ph/0306438*, 2003.

[18] C. Charmousis, E. J. Copeland, A. Padilla, and P. M. Saffin. General second-order scalar-tensor theory and self-tuning. *Physical Review Letters*, 108(5):051101, 2012.

[19] D. D. Clayton, W. A. Fowler, T. Hull, and B. Zimmerman. Neutron capture chains in heavy element synthesis. *Annals of Physics*, 12(3):331–408, 1961.

[20] T. Clifton, P. G. Ferreira, A. Padilla, and C. Skordis. Modified gravity and cosmology. *Physics Reports*, 513(1):1–189, 2012.

[21] P. Collaboration et al. Planck 2013 results. *Overview of Products and Scientific Results. arXiv*, 1303, 2013.

[22] C. R. Contaldi, T. Wiseman, and B. Withers. Teves gets caught on caustics. *Physical Review D*, 78(4):044034, 2008.

[23] B. Craps. The cosmological singularity problem. *arXiv preprint arXiv: 1001.4367*, 2010.

[24] P. Creminelli, A. Nicolis, and E. Trincherini. Galilean genesis: an alternative to inflation. *Journal of Cosmology and Astroparticle Physics*, 2010(11):021, 2010.

[25] R. H. Dicke. Mach's principle and invariance under transformation of units. *Physical Review*, 125(6):2163, 1962.

[26] R. H. Dicke, P. J. E. Peebles, P. G. Roll, and D. T. Wilkinson. Cosmic black-body radiation. *The Astrophysical Journal*, 142:414–419, 1965.

[27] P. Dunsby. An introduction to tensors and relativity. *Shiva, Cape Town*, 2000.

[28] G. Dvali, G. Gabadadze, and M. Porrati. 4d gravity on a brane in 5d minkowski space. *Physics Letters B*, 485(1):208–214, 2000.

[29] A. Einstein. Die grundlage der allgemeinen relativitätstheorie. *Annalen der Physik*, 354(7):769–822, 1916.

[30] D. J. Eisenstein and W. Hu. Baryonic features in the matter transfer function. *The Astrophysical Journal*, 496(2):605, 1998.

[31] C. Eling and T. Jacobson. Static post-newtonian equivalence of general relativity and gravity with a dynamical preferred frame. *Physical Review D*, 69(6):064005, 2004.

[32] J. W. Elliott, G. D. Moore, and H. Stoica. Constraining the new aether: Gravitational cherenkov radiation. *Journal of High Energy Physics*, 2005(08):066, 2005.

[33] G. Ellis, H. Nicolai, R. Durrer, and R. Maartens. Editorial on the grg special issue on dark energy. *General Relativity and Gravitation*, 40(2):219–220, 2008.

[34] K. Enqvist and T. Mattsson. The effect of inhomogeneous expansion on the supernova observations. *Journal of Cosmology and Astroparticle Physics*, 2007(02):019, 2007.

[35] B. Z. Foster and T. Jacobson. Post-newtonian parameters and constraints on einstein-aether theory. *Physical Review D*, 73(6):064015, 2006.

[36] A. Friedmann. 125. on the curvature of space. *Zeitschrift für Physik*, 10:377–386, 1922.

[37] A. Friedmann. Über die möglichkeit einer welt mit konstanter negativer krümmung des raumes. *Zeitschrift für Physik A Hadrons and Nuclei*, 21(1):326–332, 1924.

[38] A. H. Guth. Inflationary universe: A possible solution to the horizon and flatness problems. *Physical Review D*, 23(2):347, 1981.

[39] S. W. Hawking and R. Penrose. The singularities of gravitational collapse and cosmology. In *Proceedings of the Royal Society of London A: Mathematical, Physical and Engineering Sciences*, volume 314, pages 529–548. The Royal Society, 1970.

[40] R. W. Hellings and K. Nordtvedt Jr. Vector-metric theory of gravity. *Physical Review D*, 7(12):3593, 1973.

[41] F. B. Hildebrand. *Advanced calculus for applications*, volume 63. Prentice-Hall Englewood Cliffs, NJ, 1962.

[42] M. P. Hobson, G. P. Efstathiou, and A. N. Lasenby. *General relativity: an introduction for physicists*. Cambridge University Press, 2006.

[43] G. W. Horndeski. Second-order scalar-tensor field equations in a four-dimensional space. *International Journal of Theoretical Physics*, 10(6):363–384, 1974.

[44] T. Jacobson. Einstein-aether gravity: a status report. *arXiv preprint arXiv: 0801.1547*, 2008.

[45] J. B. Jiménez and A. L. Maroto. A cosmic vector for dark energy. *arXiv preprint arXiv: 0801.1486*, 2008.

[46] J. B. Jiménez and A. L. Maroto. Cosmological electromagnetic fields and dark energy. *Journal of Cosmology and Astroparticle Physics*, 2009(03):016, 2009.

[47] J. B. Jiménez and A. L. Maroto. Cosmological evolution in vector-tensor theories of gravity. *Physical Review D*, 80(6):063512, 2009.

[48] J. B. Jiménez and A. L. Maroto. Viability of vector-tensor theories of gravity. *Journal of Cosmology and Astroparticle Physics*, 2009(02):025, 2009.

[49] G. Jungman, M. Kamionkowski, A. Kosowsky, and D. N. Spergel. Cosmological-parameter determination with microwave background maps. *arXiv preprint astro-ph/9512139*, 1995.

[50] N. Kan, T. Maki, and K. Shiraishi. Weyl invariant dirac-born-infeld-einstein theory. *arXiv preprint arXiv: 1012.5375*, 2010.

[51] S. Kandhai. Exploring the cosmological dynamics of a viable theory for f(r)-gravity. 2014.

[52] T. Kobayashi, M. Yamaguchi, and J. Yokoyama. Generalized g-inflationinflation with the most general second-order field equations. *Progress of Theoretical Physics*, 126(3):511–529, 2011.

[53] A. Kofman. The origin of matter in the universe: Reheating after inflation astroph/9605155.

[54] T. S. Koivisto and F. R. Urban. Disformal vectors and anisotropies on a warped brane. *arXiv preprint arXiv: 1407.3445*, 2014.

[55] E. W. Kolb and M. S. Turner. The early universe. *Front. Phys., Vol. 69,*, 1, 1990.

[56] M. Kowalski, D. Rubin, G. Aldering, R. Agostinho, A. Amadon, R. Amanullah, C. Balland, K. Barbary, G. Blanc, P. Challis, et al. Improved cosmological constraints from new, old, and combined supernova data sets. *The Astrophysical Journal*, 686(2):749, 2008.

[57] M. Kunz. The phenomenological approach to modeling the dark energy. *Comptes Rendus Physique*, 13(6):539–565, 2012.

[58] K. Lake. Sudden future singularities in flrw cosmologies. *arXiv preprint gr-qc/0407107*, 2004.

[59] A. D. Linde. A new inflationary universe scenario: A possible solution of the horizon, flatness, homogeneity, isotropy and primordial monopole problems. *Physics Letters B*, 108(6):389–393, 1982.

[60] C. Ma and T.-J. Zhang. Power of observational hubble parameter data: a figure of merit exploration. *The Astrophysical Journal*, 730(2):74, 2011.

[61] R. A. Malaney and G. J. Mathews. Probing the early universe: A review of primordial nucleosynthesis beyond the standard big bang. *Physics Reports*, 229(4):145–219, 1993.

[62] C. Middleton. Newtonian and general relativistic orbits with small eccentricities on 2d surfaces. *Bulletin of the American Physical Society*, 59, 2014.

[63] R. K. Nagle, E. B. Saff, A. D. Snider, and S13/00. *Fundamentals of differential equations*. Addison-Wesley Boston, MA, 2000.

[64] A. Nicolis, R. Rattazzi, and E. Trincherini. Galileon as a local modification of gravity. *Physical Review D*, 79(6):064036, 2009.

[65] A. Nicolis, R. Rattazzi, and E. Trincherini. Energys and amplitudes positivity. *Journal of High Energy Physics*, 2010(5):1–22, 2010.

[66] K. Nordtvedt Jr. Post-newtonian metric for a general class of scalar-tensor gravitational theories and observational consequences. *The Astrophysical Journal*, 161:1059, 1970.

[67] M. Novello and S. P. Bergliaffa. Bouncing cosmologies. *Physics reports*, 463(4):127–213, 2008.

[68] A. Padilla, P. M. Saffin, and S.-Y. Zhou. Bi-galileon theory i: motivation and formulation. *Journal of High Energy Physics*, 2010(12):1–26, 2010.

[69] T. Padmanabhan. *Cosmology and astrophysics through problems*. Cambridge university press, 1996.

[70] T. Padmanabhan. Cosmological constant and the weight of the vacuum. *Physics Reports*, 380(5):235–320, 2003.

[71] R. Partridge and D. T. Wilkinson. Isotropy and homogeneity of the universe from measurements of the cosmic microwave background. *Physical Review Letters*, 18(14):557, 1967.

[72] P. J. E. Peebles. *Principles of physical cosmology*. Princeton University Press, 1993.

[73] N. J. Popławski. Cosmology with torsion: An alternative to cosmic inflation. *Physics Letters B*, 694(3):181–185, 2010.

[74] W. H. Press and P. Schechter. Formation of galaxies and clusters of galaxies by self-similar gravitational condensation. *The Astrophysical Journal*, 187:425–438, 1974.

[75] E. Recami and R. Mignani. Classical theory of tachyons (special relativity extended to superluminal frames and objects). *La Rivista Del Nuovo Cimento Series 2*, 4(2):209–290, 1974.

[76] A. G. Riess, A. V. Filippenko, P. Challis, A. Clocchiatti, A. Diercks, P. M. Garnavich, R. L. Gilliland, C. J. Hogan, S. Jha, R. P. Kirshner, et al. Observational evidence from supernovae for an accelerating universe and a cosmological constant. *The Astronomical Journal*, 116(3):1009, 1998.

[77] A. G. Riess, L. Macri, S. Casertano, H. Lampeit, H. C. Ferguson, A. V. Filippenko, S. W. Jha, W. Li, R. Chornock, and J. M. Silverman. Erratum: Determination of the hubble constant with the hubble space telescope and wide field camera 3 (2011, apj, 730, 119). *The Astrophysical Journal*, 732(2):129, 2011. http://stacks.iop.org/0004-637X/732/i=2/a=129.

[78] C. Robinson. *Dynamical systems: stability, symbolic dynamics, and chaos*. CRC press, 1995.

[79] H. H. Rosenbrock and C. Storey. *Mathematics of dynamical systems*. Nelson, 1970.

[80] B. W. Rust, D. P. Oleary, and K. M. Mullen. Modelling type 1a supernova light curves. *Exponential Data Fitting and Its Applications*, pages 169–186, 2010.

[81] D. Ryu, H. Kang, and P. L. Biermann. Cosmic magnetic fields in large scale filaments and sheets. *arXiv preprint astro-ph/9803275*, 1998.

[82] A. S. Sakharov and H. Hofer. Development of the universe and new cosmology. *arXiv preprint astro-ph/0309326*, 2003.

[83] F. Sbisà. Modified theories of gravity. *arXiv preprint arXiv: 1406.3384*, 2014.

[84] L. Smarr and J. W. York Jr. Kinematical conditions in the construction of spacetime. *Physical Review D*, 17(10):2529, 1978.

[85] D. N. Spergel, R. Bean, O. Doré, M. Nolta, C. Bennett, J. Dunkley, G. Hinshaw, N. Jarosik, E. Komatsu, L. Page, et al. Three-year wilkinson microwave anisotropy probe (wmap) observations: implications for cosmology. *The Astrophysical Journal Supplement Series*, 170(2):377, 2007.

[86] D. N. Spergel, L. Verde, H. V. Peiris, E. Komatsu, M. Nolta, C. Bennett, M. Halpern, G. Hinshaw, N. Jarosik, A. Kogut, et al. First-year wilkinson microwave anisotropy probe (wmap) observations: determination of cosmological parameters. *The Astrophysical Journal Supplement Series*, 148(1):175, 2003.

[87] N. Straumann. The history of the cosmological constant problem. *arXiv preprint gr-qc/0208027*, 2002.

[88] M. Tegmark, M. A. Strauss, M. R. Blanton, K. Abazajian, S. Dodelson, H. Sandvik, X. Wang, D. H. Weinberg, I. Zehavi, N. A. Bahcall, et al. Cosmological parameters from sdss and wmap. *Physical Review D*, 69(10):103501, 2004.

[89] D. Terr. The big bang theory.

[90] D. Tytler, X.-m. Fan, and S. Burles. The cosmological baryon density from the deuterium abundance at a redshift z= 3.57. *arXiv preprint astro-ph/9603069*, 1996.

[91] L. F. Urrutia. Corrections to flat-space particle dynamics arising from space granularity. In *Special Relativity*, pages 299–345. Springer, 2006.

[92] J.-P. Uzan, C. Clarkson, and G. F. Ellis. Time drift of cosmological redshifts as a test of the copernican principle. *Physical Review Letters*, 100(19):191303, 2008.

[93] R. A. Vanderveld, E. E. Flanagan, and I. Wasserman. Mimicking dark energy with lemaitre-tolman-bondi models: Weak central singularities and critical points. *Physical Review D*, 74(2):023506, 2006.

[94] P. Vitebsky. From cosmology to environmentalism: shamanism as local knowledge in a global setting. *Shamanism: A Reader*, 276, 2003.

[95] M. Von Laue. *Die Relativitätstheorie*, volume 1. F. Vieweg & sohn, 1921.

[96] R. V. Wagoner. Scalar-tensor theory and gravitational waves. *Physical Review D*, 1(12):3209, 1970.

[97] R. M. Wald. *General relativity*. University of Chicago press, 2010.

[98] T. P. Walker, G. Steigman, H.-S. Kang, D. M. Schramm, and K. A. Olive. Primordial nucleosynthesis redux. *Astrophysical Journal*, 376:51–69, 1991.

[99] S. Weinberg. Gravitation and cosmology: Principle and applications of general theory of relativity. 1972.

[100] S. Weinberg. The cosmological constant problem. *Reviews of Modern Physics*, 61(1):1, 1989.

[101] S. Weinberg. *The first three minutes: a modern view of the origin of the universe*. Basic Books, 1993.

[102] S. Weinberg. *Cosmology*. Oxford Univ. Press, 2008.

[103] C. Wetterich. Cosmology and the fate of dilatation symmetry. *Nuclear Physics B*, 302(4):668–696, 1988.

[104] S. Wiggins. *Introduction to applied nonlinear dynamical systems and chaos*, volume 2. Springer Science & Business Media, 2003.

[105] C. M. Will and K. Nordtvedt Jr. Conservation laws and preferred frames in relativistic gravity. i. preferred-frame theories and an extended ppn formalism. *The Astrophysical Journal*, 177:757, 1972.

[106] J. L. Willems. *Stability theory of dynamical systems*. Nelson, 1970.

[107] B. Withers. Einstein-aether as a quantum effective field theory. *Classical and Quantum Gravity*, 26(22):225009, 2009.

[108] K. K. Wu, O. Lahav, and M. J. Rees. The large-scale smoothness of the universe. *Nature*, 397(6716):225–230, 1999.

[109] I. B. Zeldovich and I. D. Novikov. *Relativistic Astrophysics, 2: The Structure and Evolution of the Universe*, volume 2. University of Chicago Press, 1971.